2007

A putative approach for influencing stomatal density by over-expressing NADP-dependent malic enzyme in arabidopsis

Michael M. Gabor

A PUTATIVE APPROACH FOR INFLUENCING STOMATAL DENSITY BY OVER-EXPRESSING NADP-DEPENDENT MALIC ENZYME IN ARABIDOPSIS

by

Michael M. Gabor

Thesis

Submitted to the Department of Biology

Eastern Michigan University

in partial fulfillment of the requirements

for the degree of

MASTER OF SCIENCE

in

Molecular and Cellular Biology

Thesis Committee:

Dr. Marianne Laporte, Chair

Dr. Steven Pernecky, Member

Dr. Glenn Walker, Member

Dr. Robert Winning, Member

June 15, 2007

Ypsilanti, Michigan

DEDICATION

To my precious family: Marin, Angela, Melissa, Phillip, and Joshua Gabor

ACKNOWLEDGEMENTS

Many times, it seems as if the simply said words “thank you” are not sufficient in conveying gratitude and appreciation; however, I still wish to acknowledge the many persons whom made this study a success. First and foremost, I would like to sincerely thank my advisor, Dr. Marianne Laporte, for her constant support, guidance, patience, and encouragement, which all allowed me to reach this point of completion and success. I would also like to thank my committee members, Dr. Steven Pernecky, Dr. Glenn Walker, and Dr. Robert Winning, all of whom had a profound impact on my undergraduate and graduate career.

Many of my colleagues contributed much in making this study a success, and my acknowledgment would not be complete without thanking them. My gratitude goes to Christine Notis for her RT-PCR, 35S Arabidopsis transgenic plant, and enzyme activity contributions to this study. I sincerely thank Pooja Thakur for her KAT2 Arabidopsis transgenic plant contribution to this study. I also thank Erik Rowley and Alina Terzulli for the limit of detection for the immunoblotting procedure and the NADP-ME positive control, respectively.

I would like to thank my parents, Marin and Angela, and my siblings, Melissa, Phillip, and Joshua, for their constant support during my educational career. I love them all very much.

Finally and most importantly, I wish to thank Almighty God for giving me the strength, guidance, courage, and hope during this sometimes difficult journey. He made Proverbs 3:5-6 a reality for me.

ABSTRACT

Stomata are leaf structures critical for plant survival because they modulate the rate of transpiration. This study will examine a possible mode for regulating stomatal density by over-expressing NADP-dependent malic enzyme (NADP-ME), which is thought to deplete the counter-anion pool in Arabidopsis thaliana guard cells. It was hypothesized that over-expressing NADP-ME in Arabidopsis will elevate stomatal density. Scanning electron microscopy was employed to determine if any differences exist in numbers of stomatal complexes among transgenic lines and wild-type Arabidopsis. The results indicated a significant increase in stomatal numbers among some transgenic plant lines relative to the wild-type. Second, a series of molecular tests were utilized to provide NADP-ME activity and transgene expression evidence. These included western blots, tissue assay blots, enzyme activity assays, and RT-PCR reactions. Altering NADP-ME expression levels may present a putative approach for influencing stomatal development.

TABLE OF CONTENTS

LIST OF FIGURES

INTRODUCTION

With each passing year, global energy and food demands increase at phenomenal rates. Estimates indicate that at current fossil fuel production and consumption rates, current oil, natural gas, and coal reserves will last for approximately 41, 64, and 155 years, respectively (British Petroleum, 2006). To reduce dependence on fossil fuels, the United States and the European Union are directing tremendous resources towards producing energy from plant-derived sources such as corn grains, sugar cane, and beets (Himmel et al., 2007).

Plants supply about 90% of the global human caloric intake (Chawla, 2002) and the growing global population will continue to strain agricultural resources. Both the growing energy and food needs are greatly fueling the development of improved agricultural techniques and methods. A plethora of genetically engineered plants, *i.e.* transgenic plants, has been developed with resistance to pathogens and viral infections, and to even produce fruit with a longer shelf life (Chawla, 2002). Yet the greatest advancements in plant genetic engineering are still on the horizon.

One limiting reagent for greatly increasing agricultural yields is water. In fact, nearly 70% of globally available water is used by agriculture (Chaves and Oliveria, 2004), making the management of fresh water resources a major challenge. Previous practices to improve agricultural production included improved irrigation techniques and methods, but these alone were insufficient. Researchers are now genetically engineering plants from a physiological and molecular basis (Chaves and Oliveria, 2004) in order to develop plants with improved drought tolerance, drought avoidance, or water-use efficiency. Recently, a novel approach to reducing stomatal conductance and therefore improving

water use efficiency has been proposed by manipulating guard cell anion metabolism (Laporte et al., 2002). This approach reduces stomatal aperture and conductance while maintaining stomatal responses to environmental stimuli. When applied, plants may gain improved water use efficiency under irrigation and may increase agricultural yields for both food and energy production.

Stomata and Transpiration

To limit water loss, land plants developed a waxy layer, called the cuticle, impermeable to gas exchange on aerial tissue (Roelfsema and Hedrich, 2005). However, a mechanism to allow for gas exchange between plants and the atmosphere was required, which drove the evolution of stomata. Stomata are present on aerial tissue, predominant on leaves, but may also be found on petioles, the stem, and primary roots (Christodoulakis et al., 2002) in certain plant species. Epidermal tissue and a pair of guard cells define the stomatal pore's aperture (Boudolf et al., 2004).

Stomatal pores, acting as a "watergate" (Roelfsema and Hedrich, 2005), open to make carbon dioxide available for photosynthesis, while forfeiting water. The plant stoma facilitates nearly 95% of a plant's water loss to the atmosphere by transpiration (Schroeder et al., 2001). As water osmotically enters and increases guard cell volume, they swell and bow apart, enlarging the stomatal aperture (Roelfsema and Hendrich, 2005). Stomata are critical for plant survival for they orchestrate the exchange of intracellular gases required for photosynthesis with the atmosphere, while limiting the cost of water loss via transpiration (Blatt, 2000).

Stomatal Development

A fundamental understanding of stomatal development is key to comprehending the regulation of stomatal behavior via plant biotechnology. The regulation of stomatal development may usher in new approaches to supplement and succeed today's plant genetic engineering techniques for agricultural and energy production applications. Stomatal development is quite complex because it intertwines both environmental and cellular communication signals. Understanding of stomatal development is still not complete, but major advances have been made in deciphering this phenomenon in Arabidopsis (*Arabidopsis thaliana)*. Arabidopsis consists of a simple epidermis made of three major cell types: stomatal guard cells, pavement cells, and trichomes (Bergmann, 2004).

Stomatal Development Pathway

Stomatal development is much more complex in dicots, such as Arabidopsis, than in monocots. In dicots, stomatal development and leaf extension occur simultaneously, resulting in a leaf composed of stomata at different developmental stages (Croxdale, 2000).

Nadeau and Sack (2003) report that stomatal positioning requires at least one pavement cell in between two stomatal complexes, *i.e.* a one-cell-spacing rule. This strict distribution optimizes the efficiency of gaseous diffusion shells, evapotranspiration, ion exchange required for vacuolar osmolarity, and the ratio between carbon dioxide uptake and photosynthetic activity.

Several mechanisms exist to maintain normal stomatal development. Bergmann describes three critical developmental features for stomatal complexes. Stomatal

development utilizes symmetrical and asymmetrical divisions of stomatal pre-cursor cells. During development, neighboring epidermal cells release signals to provide a local pattern preventing two adjacent stomatal complexes from developing. Finally, environmental cues may influence overall stomatal numbers (Bergmann, 2004).

Stomatal development is completely post-embryonic, beginning within a day after seed germination (Bergmann, 2004). During stomatal complex formation, the number and orientation of cell divisions are both critical for correct stomatal patterning (von Groll et al., 2002*)*. Nadeau and Sack indicate that during Arabidopsis stomatal development, there is an initial stem cell commitment step to the stomatal pathway. Meristemoid cells can undergo multiple rounds of asymmetrical cell division because of their stem cell-like activity. Initiation begins with the determination of a meristemoid mother cell, which then asymmetrically divides to produce a smaller meristemoid and a larger neighbor cell (Nadeau and Sack, 2003; Fig. 1). A cell adjacent to a stoma or a precursor cell is termed a neighbor cell. Then the meristemoid cell asymmetrically divides (Paliwal, 1967) to regenerate a meristemoid cell and an additional neighbor cell, thereby following the one-cell-spacing rule. Nadeau and Sack specify that then the neighbor cell asymmetrically divides, serving as a meristemoid mother cell, to produce a smaller cell that is termed a satellite meristemoid cell (to emphasize this class of cell division producing the one-cell spacing requirement) and another neighbor cell. Then each meristemoid develops into a guard mother cell that symmetrically divides to form a stoma. A second type of terminally differentiated epidermal cell, termed a pavement cell, also develops via asymmetrical divisions (Nadeau and Sack, 2003; Fig. 1). The presence

of pavement cells in between stomatal complexes is critical for ion exchange between guard cells and pavement cells (Wang et al., 2006).

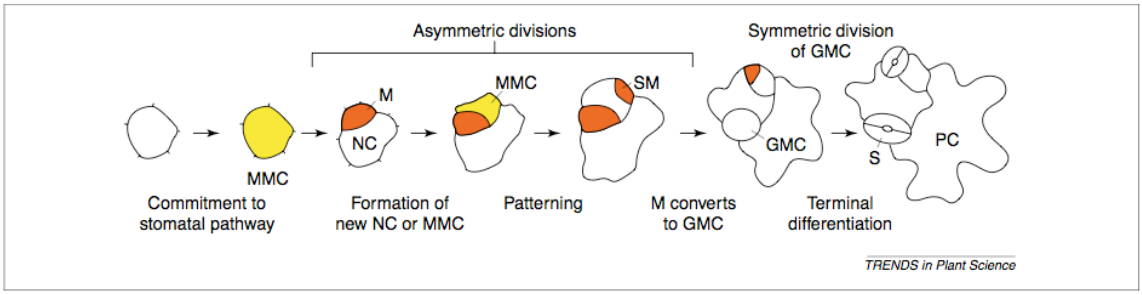

Figure 1. A proposed pathway for stomatal development in Arabidopsis. Initiation takes place with the selection of a meristemoid mother cell (MMC, yellow), which asymmetrically divides to generate a larger neighbor cell or precursor cell (NC) and a smaller meristemoid cell (M, red). Asymmetrical meristemoid cell division regenerates a meristemoid and produces another NC. This new NC functions as a MMC. Then this MMC asymmetrically divides to produce a NC and the smaller cell is called a satellite meristemoid (SM, red) to emphasize this class of cell division producing the one-cell spacing requirement. Then each M becomes a guard mother cell (GMC), which divides symmetrically to produce a stoma (S). Pavement cells (PC), another class of terminally differentiated epidermal cells, form via asymmetrical divisions. From Nadeau and Sack, 2003.

A fundamental feature of stomatal patterning is the maintenance of the one-cell-spacing rule. Nadeau and Sack specify that the orientation of the asymmetric divisions in neighbor cells is responsible for determining the stomatal patterning. The neighbor cell's plane is orientated in such a way to prevent contact between the preexisting stoma or precursor and new satellite meristemoids (Nadeau and Sack, 2003).

Gene Regulation of Stomatal Development

Stomatal development is highly regulated through a series of molecular switches, receptors, and proteases (Figure 2). Analyzing mutations in key stomatal developmental genes has greatly advanced the understanding of this phenomenon. Stomatal patterning genes, encoding FOUR LIPS (FLP) and TOO MANY MOUTHS (TMM), were first discovered, and mutations in these genes caused stomatal clustering (Nadeau and Sack,

2002). FLP encodes a R2R3 MYB-type transcription factor (Ohashi-Ito and Bergmann, 2006), which is required for meristemoid to guard cell progression (Lai et al., 2005) and acts as a negative regulator later in stomatal development (Nadeau and Sack, 2002, Fig. 2).

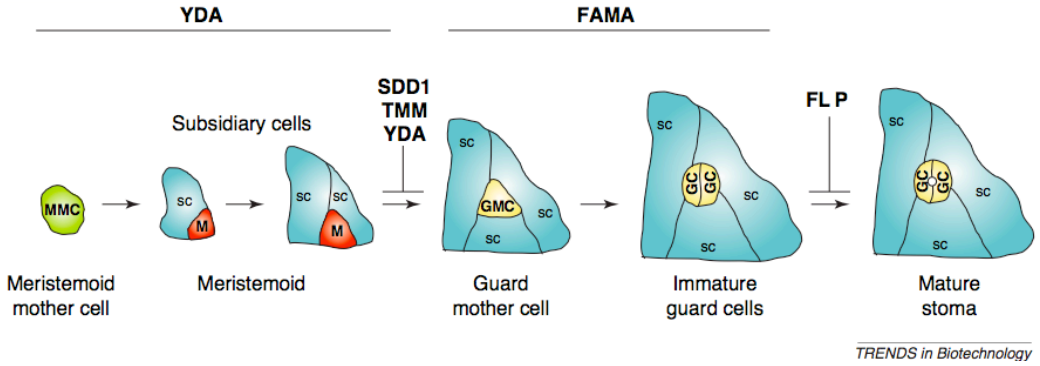

Figure 2. Proposed gene regulation pathway of stomatal development. SDD1 (STOMATAL DENSITY AND DISTRIBUTION1), TMM (TOO MANY MOUTHS), FLP (FOUR LIPS), YDA (Mitogen-Activated Protein Kinase Kinase Kinase), and FAMA gene products control stomatal development. See text for explanation. Abbreviations: meristemoid mother cell (MMC), meristemoid (m), subsidiary sell (sc), guard mother cell (gmc), guard cell (gc). From Chaerle et al., 2005.

Nadeau and Sack indicate that TMM has been found to control the plane and number of NC divisions. The *tmm* mutant produces extra meristemoids, which are placed adjacent to preexisting stomata or precursors, thereby generating clustered stomata. TMM is expressed in meristemoids, guard mother cells, and their recent sister cells. Based on subcellular localization of green fluorescent protein, TMM is located in the cell membrane (Nadeau and Sack, 2003), thereby functioning as a putative cell surface receptor (Chaerle et al., 2005). A leucine-rich repeat receptor-like protein (LRR-RLP) is encoded by TMM, and like other LRR-RLPs, TMM has no cytoplasmic kinase, thereby relying on other unknown factors to contribute to the intracellular signaling pathway (Nadeau and Sack, 2003; Fig. 2).

It has been suggested that the SDD1 (STOMATAL DENSITY AND DISTRIBUTION1) gene product may interact with TMM (Berger and Altmann, 2000). SDD1 encodes a subtilisin-like serine protease and may be involved in stomatal developmental signal processing (Coupe et al., 2006). Nadeau and Sack report that SDD1 is similar to proteases found in animal cells and thereby functions in signaling by modifying or cleaving a developmental ligand. Experiments indicate that SDD1 is secreted because GFP-SDD1 fusion proteins localize near the cell membrane, even though it lacks an appropriate transmembrane region or motif. The localization of SDD1 may be due to association with the cell membrane by a protein complex or by a membrane-bound substrate. SDD1 is expressed in meristemoids and guard mother cells (Nadeau and Sack, 2003).

Phenotypic analysis of the *sdd1* and *tmm* mutants indicate a probable role for each gene. Fig. 3 indicates that both the *sdd1* and *tmm* mutants have more stomata relative to the wild-type. However, *sdd1* adheres to the one-cell-spacing rule more closely, as it contains far fewer stomatal complex clusters than *tmm* (Fig. 3C and 3B, respectively).

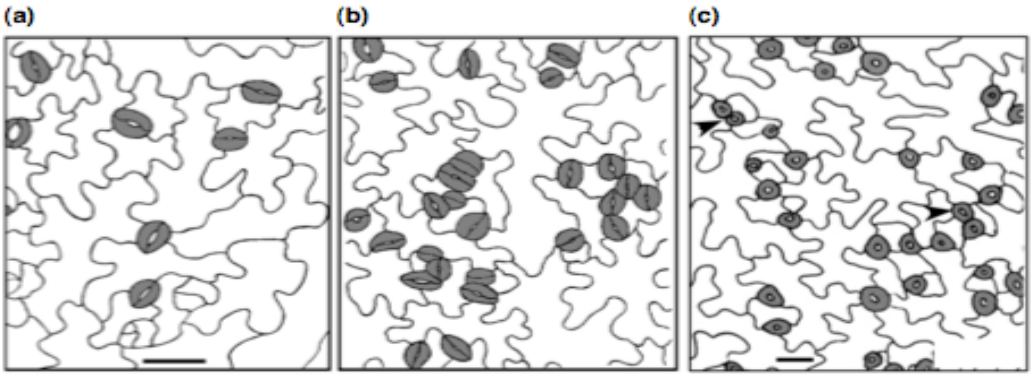

Figure 3. Phenotype analysis illustrating the effects of stomatal development gene mutations. A, Wild-type Arabidopsis. B, *too many mouths (tmm)* mutant. C, *stomatal density and distribution1 (sdd1)* mutant. From Nadeau and Sack, 2003.

As a result, both genes are negative regulators of neighbor cell division, prevent asymmetric division in cells not following the one-cell spacing rule, and encourage meristemoid division by delaying transition to guard mother cells (Fig. 2). TMM is thought to be more important in stomatal patterning and SDD1 more important for limiting density (Nadeau and Sack, 2003). It is hypothesized that stomatal precursor cells may transmit an SDD1 signal, that might transform or interact with an unknown ligand, and then the unknown ligand may bind to a receptor complex composed of TMM. The TMM receptor complex may then determine the polarity that directs the plane of neighbor cell division or may act to limit the number of neighbor cell divisions, as indicated in Fig. 4 (Nadeau and Sack, 2003).

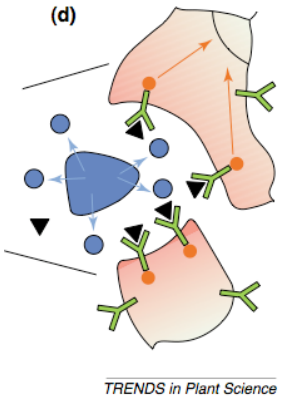

Figure 4. Proposed pathway for SDD1 and TMM signaling pathway. Precursor stomatal cell (blue) may secrete an SDD1 gene product (blue circles) that may alter or interact with an unknown ligand (black triangles). The unknown ligand and the SDD1 gene product then bind to the TMM receptor complex (green). The TMM receptor complex may then determine the polarity that directs the plane of neighbor cell division or may act to limit the number of neighbor cell divisions. From Nadeau and Sack, 2003.

YODA (YDA), upstream of SDD1, TMM, and FLP, is designated as a cell-fate switch, acting as a key regulator of stomatal development and patterning (Chaerle et al., 2005, Fig. 2). YDA is mitogen-activated protein kinase kinase kinase (MAPKKK), which integrates environmental responses with stomatal development in order to determine the optimal differentiation proportion of stomata versus pavement cells in leaf epidermis (Wang et al., 2007).

At the critical transitory stage from guard mother cell proliferation to stoma, FAMA controls the final proliferation to differentiation switch during stomatal development (Fig. 2). Ohashi-Ito and Bergmann report that FAMA encodes a putative basic helix-loop-helix transcription factor required for arresting cell division and promoting guard cell differentiation. It was shown that when Arabidopsis, with loss-of-function mutations in the negative regulators SDD1, TMM, and YODA, were combined with a FAMA mutation, guard cells were not produced. Therefore, FAMA acts as the master regulator of stomatal differentiation (Ohashi-Ito and Bergmann, 2006).

Environmental Signals Regulating Stomatal Development

To complement stomatal development understanding, determining how environmental factors influence stomatal development is necessary to enhance plant genetic engineering techniques. It has been established that atmospheric CO_2 partial pressure and light intensity interdependently act as two environmental signals to regulate stomatal numbers and subsequently stomatal development (Coupe et al. 2006). In Arabidopsis, elevated CO_2 levels decreased stomatal density (Teng et al., 2006). Previous research demonstrated that mature leaves measure CO_2 levels by an unknown mechanism and broadcast a stomatal developmental signal directing development in young leaves (Lake

et al., 2001). Hence, mature leaves detect environmental signals and transfer this information to younger leaves via an unknown signal(s), thereby aligning stomatal development with environmental conditions (Coupe et al. 2006). By using mature leaves to detect environmental signals, versus younger, unfurled leaves developing in a less representative environment, a plant optimally measures environmental conditions (Larcher, 1995) and fine-tunes stomatal density.

Biological and Environmental Signals Regulating Stomatal Movements

A central goal for increased plant water use efficiency is to decrease stomatal conductance by reducing stomatal aperture, and new insights may be gained by studying the influence of environmental signals on stomatal behavior. Guard cells, which form the stomatal pore, receive environmental signals, such as light intensity, water deficit, and CO_2 concentrations, and integrate them with endogenous signals in order to optimize stomatal movements (Schroeder et al., 2001). Light signals for stomatal opening in order to increase CO_2 uptake for photosynthesis (Roelfsema and Hedrich, 2005). Stomata respond to both red and blue light with great wavelength specificity, making blue light more effective than red light in most species (Willmer and Fricker, 1996). An electrogenic guard cell plasma membrane proton pump is activated and initiates stomatal opening upon signaling from the blue light photoreceptor.

However, light signaling for stomatal opening is not independent but is integrated with other inputs, such as water deficit, to act in an antagonistic manner on stomatal aperture (Roelfsema and Hedrich, 2005). During drought conditions, roots release abscisic acid (ABA), a plant hormone, which travels via the xylem stream to act on guard cells (Schroeder et al., 2001). This water deficit signal induces stomatal closure or prevents

stomatal opening in order to limit water lost via transpiration (Roelfsema and Hedrich, 2005).

Carbon dioxide concentration levels are another environmental signal that acts in concert with the others to modulate stomatal movements. Elevated CO_2 levels induce CO_2-senstive stomata to close, whereas low levels open them (Hedrich et al., 2001). Guard cells are believed to sense CO_2 levels because they optimize water use efficiency by gauging mesophyll CO_2 requirements while monitoring water status (Vavasseur and Raghavendra, 2005). Studies of guard cell protoplasts indicated that CO_2 sensing is inherent to guard cells (Fitzsimons and Weyers, 1986), and it was later observed that guard cells respond to intracellular CO_2 concentration by monitoring the mesophyll assimilation rate (Mott, 1988). When plants were not under a water deficit, it was determined that doubling atmospheric CO_2 levels above ambient resulted in a 40% reduction in stomatal conductance (Morison, 1987).

Hedrich et al. (2001) report that light is not needed for the observed stomatal responses to CO_2 levels. This response is maintained in the dark because plants store fixed CO_2 as malate in vacuoles and when released, it enters leaf apoplasts where it is metabolized by malic enzyme to release CO_2 and pyruvate. It was observed, via patch-clamp studies, that as CO_2 levels increased, so did apoplastic malate levels. This led to the development of the somewhat controversial "malate hypothesis," which proposed that heightened CO_2 levels signal the release of malate from guard and mesophyll cells. Malate then triggers Cl^- and malate-permeable anion channels, causing anion release. Guard cell cation release follows, eliciting a loss in turgor, and subsequential stomatal closure.

Guard Cell Control of Stomatal Aperture

Guard cell control of stomatal aperture depends upon the concentration of osmotically active ions, which determine turgor pressure and volume. During stomatal opening, guard cells need to increase their plasma membrane surface by almost 40%, most likely accomplished by vesicle fusion with the plasma membrane (Roelfsema and Hedrich, 2005). The guard cell volume is determined by the transport of ions into the cell's vacuole with water osmotically following (Heldt, 2005).

Guard cells have highly specialized ion transporters because, unlike in different plant tissue, ion transport occurs in both directions to allow for stomatal opening and closing (Roelfsema and Hedrich, 2005). To facilitate stomatal opening, blue light activates P-type ATPase proton pumps, which extrude protons from the cytoplasm of the cell in order to generate a proton motive force responsible for driving solute flow (Heldt, 2005). Once the membrane is hyperpolarized, voltage-dependent, inward-rectifying K^+ channels open, to allow positive K^+ ions to passively enter (Roelfsema and Hedrich, 2005). Stomatal movement depends heavily upon on the uptake of K^+ (Fisher, 1968), making it the dominant cation accumulated in guard cells during stomatal opening (Schroeder et al., 1994). In addition, a proton motive force, coupled to an H^+-coupled symport system, is used to drive the influx of Cl^- (MacRobbie, 1987), in order to counter the influx of K^+, and glucose (Heldt, 2005). Malate $^{2-}$, another anion of significant importance (Roelfsema and Hedrich, 2005) accumulates in high concentrations to counter the influx of K^+ (Outlaw and Lowry, 1977; Raschke and Schnabl, 1978).

During stomatal opening, there is both a malate influx in guard cells from the apoplast (Ritte and Raschke, 2003) and production of malate in large amounts (Raschke et al.,

1988) by glycolytic degradation of starch stored in guard cell chloroplasts. Specifically, starch is degraded to phosphoenolpyruvate, which is then converted to oxaloacetate by phosphoenolpyruvate carboxylase in the cytoplasm. Then oxaloacetate is reduced to malate in the chloroplast and finally accumulates in the vacuoles during stomatal opening, as indicated in Fig. 5 (Heldt, 2005).

Next, ions are sequestered in guard cell vacuoles, with water osmotically following. Protons from the guard cell vacuole are transported into the cell's vacuole via an H^+-V-ATPase (Heldt, 2005) in order to drive the influx of K^+ into the vacuole by an H^+-coupled antiport system (Roelfsema and Hedrich, 2005). A vacuole accumulation of potassium ions induces a potential difference across the vacuolar membrane (Heldt, 2005), driving the influx of organic anions from the cytosol, predominantly malate, and chloride into the vacuole (Gotow et al., 1985; Pei et al., 1996). As the concentration of ions inside the vacuole increases, water osmotically enters, causing guard cells to bow apart and enlarge as turgor pressure and volume increase, Fig. 5 (Mott et al., 2000).

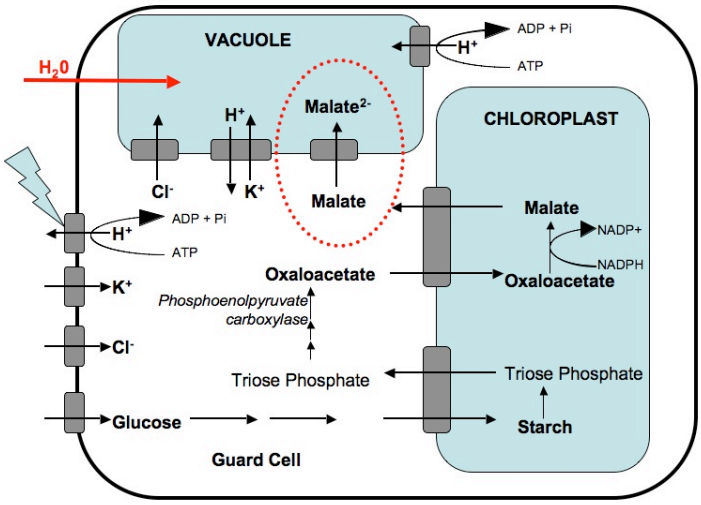

Figure 5. Stomatal biochemistry during stomatal opening. The accumulation of ions occurs in the guard cell vacuole, causing water to osmotically enter the vacuole, and subsequent stomatal opening. Malate, the principal counter-anion, is synthesized in the chloroplast. See text for more details. After Heldt, 2005.

Stomatal closure can occur more quickly than stomatal opening because it does not rely on the active transport of ions but on passive diffusion to drive solute transport down its concentration gradient (Roelfsema and Hedrich, 2005). Stomatal closure initiates when outward rectifying potassium channels transport K^+ ions out of the vacuole into guard cells (MacRobbie, 1997).

There are three main types of K^+- channels found in the plant plasma membrane: outward- rectifying channels, inward- rectifying channels, and the less common, voltage-dependent channels. Outward- and inward-rectifying channels have the physiological roles to extrude and uptake K^+ ions during stomatal closure and opening, respectively (Roelfsema and Hedrich, 2005). Genes of the *Shaker* family encode for inward-rectifying plant plasma membrane potassium channels, and GORK specifically encodes the outward-rectifying channels (Ache et al., 2000). Any disruption of GORK caused complete loss of the outward-rectifying K^+ channels (Hosy et al., 2003). In contrast to outward-rectifying channels, inward-rectifying K^+ channels are encoded by the properties of at least 5 genes (Szyyroki et al., 2001), including KAT1 (Anderson et al., 1992), AKT1 (Sentenac et al., 1992), KAT2 (Pilot et al., 2001), AtKC1 (Reintanz et al., 2002), and AKT 2/3 (Marten et al., 1999; Lacombe et al., 2000). While all genes of the *Shaker* family encode for inward-rectifying plant plasma membrane proteins, KAT1 and KST1 are extensively expressed in guard cells (Muller-Rober et al., 1995; Nakamura et al., 1995) and KAT2 is also expressed in the guard cell but at lower levels than KAT1 and KST1 (Pilot et al., 2001; Szyoki et al., 2001).

With outward K^+-rectifying channels open, the vacuolar membrane becomes depolarized, driving the efflux of anions through anion-permeable channels (Roelfsema

and Hedrich, 2005). These anion channels are permeable to malate (Hedrich, et al., 1994; Schmidt and Schroeder, 1994) and may extrude malate from guard cells (Van Krik and Rashke, 1978), and/or a NADP-malic enzyme (ME) isoform may convert malate to pyruvate in guard cells and/or epidermal cells (Outlaw et al., 1981). With the loss of solutes, water osmotically exits the vacuole, causing a loss in turgor pressure and subsequent stomatal closure.

Several lines of evidence putatively support the hypothesis that during stomatal closure, an isoform of ME, localized in guard cells and peripheral tissue, may degrade malate (Outlaw et al., 1981). Wheeler et al. (2005) determined that in Arabidopsis, different NADP-ME isoforms have activity that is more specific in leaves relative to other plant parts, suggesting a role in stomatal movements. NADP-ME activity levels were found to be higher in *Vicia* leaflet guard and epidermal cells versus photosynthetic parenchyma (Outlaw et al., 1981), again suggesting a role in stomatal movements.

NADP-Dependent Malic Enzyme

Malic enzymes (ME) are extensively found throughout nature, being employed by fungi, bacteria, plants, and animals. There are numerous ME isoforms that are found in eukaryotic cytosol, mitochondria, and/or chloroplasts. MEs are widely utilized in many metabolic pathways, depending on the enzymes' cellular localization because their products support numerous biological pathways (Lance and Rustin, 1984). MEs carry out an oxidative decarboxylation reaction, in the presence of a bivalent metal ion, of L-malate to produce CO_2, pyruvate, and NADPH (Chang and Tong, 2003).

$$\text{Malate} + NADP^+ \rightarrow \text{Pyruvate} + NADPH + CO_2 \quad [1]$$

MEs are classified according to the necessary cofactors they require, either NAD or NADP (Detarsio et al., 2003). In plants, NADP-dependent MEs (NADP-ME) are located in plastids and the cytosol (Edwards and Andreo, 1992; Drincovich et al., 2001) and NAD-dependent ME's main role in mitochondria is to produce pyruvate for utilization in the tricarboxylic acid cycle (Artus and Edwards, 1985).

The various NADP-ME isoforms are sublocalized in multiple locations throughout plants. They have been found to function in both photosynthetic and non-photosynthetic tissue. Photosynthetic isoforms are localized in some C_4 plant bundle sheath chloroplasts and in the cytosol of some CAM plants, and non-photosynthetic isoforms are located in C_3, C_4, and CAM plant tissue (Wheeler et al., 2005).

Even though NADP-ME has been determined to function in C_4 and CAM photosynthesis, its biological role is still not fully understood. Non-photosynthetic plastidic isoforms are thought to be apart of the plant defense response (Casati et al., 1999) and lipid biosynthesis (Smith et al., 1992). Cytosolic isoforms have been determined to contribute to the plant defense response (Schaaf et al., 1995), to lignin biosynthesis (Schaaf et al., 1995), and to regulate the cytosolic pH by equilibrating malate synthesis and degradation (Martinoia and Rentsch, 1994).

In addition to the proposed metabolic roles of NADP-ME in C_3 and C_4 plants, it has been suggested to also influence the biochemistry of stomatal movements (Outlaw et al., 1981; Laporte et al., 2002). Immunolocalization evidence indicates that a cytosolic NADP-ME isoform is present in wheat (a C_3 plant) guard cells (Maurino et al., 1997), suggesting that this guard cell cytosolic ME converts malate to pyruvate during stomatal closure (Outlaw et al., 1981).

It has been shown that over-expressing NADP-ME in tobacco via a mannopine synthase promoter, which is present in guard cells and other cells, caused decreased stomatal conductance relative to wild-type tobacco. It is hypothesized that malate metabolism, caused by over-expressing NADP-ME, depletes the counter-anion pool and alters the chemiosmotic equilibrium in the vacuole, inducing subsequent stomatal closure (Laporte et al., 2002). Over-expressing NADP-ME in transgenic plants suggested an attractive mechanism for improved water-use-efficiency because the plants were still susceptible to environmental stimuli, experienced less stomatal conductance during simulated hot and dry conditions, and used water more efficiently without compromising plant growth when compared to wild-type plants (Laporte et al., 2002).

Present Study

This present research will expand malic enzyme's important application for genetically engineering plants with improved water use efficiency, by modulating stomatal movements, to also include a novel role in influencing stomatal development. This study will utilize previously generated transgenic Arabidopsis plants with elevated guard cell specific NADP-ME or elevated whole plant NADP-ME expression. Studying guard cell biased metabolism of malate is critical to determine malate's role in stomatal movements. Arabidopsis is a model organism for plant biology because its genome has been completely sequenced, it is quickly grown, and it is easily transformed.

This research will continue to analyze transgenic Arabidopsis plants with targeted NADP-ME expression in guard cells. The C_4 NADP-ME from maize leaves, which has been extensively studied, was used (Drincovich et al., 2001). Specifically, a KAT2 promoter was cloned and used to direct maize NADP-ME expression in Arabidopsis

guard cells. In addition, it was determined that the enzyme remained active at the guard cell pH 7.35, relative to its native chloroplast pH 8.0 (Thakur, 2006).

The KAT2 promoter has been previously well-characterized and found to drive expression in guard cells of all plant aerial organs. Like KAT1, KAT2 also encodes inward-rectifying K^+ channels but at lower levels, making it a weaker promoter. However, KAT2 was chosen over KAT1 because in mature leaves, KAT2 activity was primarily detected in guard cells, minor veins, and never in roots (Pilot et al., 2001).

Scanning electron microscopy (SEM) was employed to determine if over-expressing NADP-ME in Arabidopsis guard cells had any affect on either stomatal morphology or density. It has been shown that elevated NADP-ME activity may adversely affect the development of bundle sheath chloroplasts in C_4 plants and increased maize NADP-ME expression levels in transgenic rice also indicated an abnormal structure (Takeuchi et al., 2000).

A preliminary investigation was conducted on KAT2 transgenic Arabidopsis to assess both morphology and stomatal density relative to the wild-type. The results indicated no morphological differences between wild-type and transgenic Arabidopsis, but stomatal density was greatly elevated in the KAT2 transgenic lines relative to wild-type Arabidopsis. These data suggested that a more thorough stomatal density investigation of the KAT2 transgenic plants was required.

The stomatal count investigation expanded to include leaves at different developmental stages and the analysis of a second category of transgenic Arabidopsis plants. This second category of transgenic plants analyzed utilized a 35S promoter to direct maize NADP-ME expression constitutively in Arabidopsis. The 35S promoter is

derived from a common plant virus, cauliflower mosaic virus (CaMV), and is the most often utilized promoter to induce transgene expression in plants (Sunilkumar, 2002). The 35S promoter is commonly believed to be a constitutive promoter (Odell et al., 1985); however, some studies indicate that it may not express in all plant cell and tissue types (Benfey and Chua, 1989; Yang and Christou, 1990; Terada and Shimamoto, 1990; Williamson et al., 1989). In addition, its expression profile is not fully characterized in all possible cell and tissue type expressions, and expression characteristics during early developmental stages are still lacking (Sunilkumar, 2002). A recent study on the expression profile of the 35S promoter in cotton indicated that its activities were regulated during embryogenesis and beyond that, it was expressed at various levels in most cell and tissue types (Sunilkumar, 2002).

In addition to the SEM investigation, providing enzyme activity and transgene expression evidence was another objective of this study. A spectrophotometric assay was utilized to detect the production of NADPH by indicating an increase in absorbance at 340 nm (Laporte et al., 2002) in order to confirm that NADP-ME is active in the transgenic Arabidopsis. In addition, a tissue blot assay was utilized to detect the presence and activity of NADP-ME in crude protein extracts (Wheeler et al., 2005). Using anti-his antibodies, western blots were preformed, to detect the histidine-tagged maize ME in crude protein extracts.

Hypothesis

This study will continue to analyze and elucidate the effects of over-expressing NADP-ME in transgenic Arabidopsis with either a KAT2 promoter directing expression in guard cells or a 35S promoter driving constitutive expression. This study was built on

previous research indicating altered stomatal function in transgenic tobacco with an engineered constitutive expression of maize NADP-ME (Laporte et al., 2002). Observing the effects of different NADP-ME expression levels and patterns allow for a better determination of the impact of NADP-ME on stomatal behavior. Based on preliminary SEM data, it was hypothesized that elevated, KAT2-directed expression of maize NADP-ME activity will not affect stomatal morphology but may elevate stomatal density by altering stomatal biochemistry. Neither malate nor NADP-ME has been shown to influence stomatal density and may present a novel approach for influencing stomatal development. To expand the KAT2 transgenic plant analysis, transgenic 35S plants were also studied to determine if different expression levels and patterns affect stomatal density. It was hypothesized that constitutive expression of NADP-ME would elevate stomatal density. These hypotheses were addressed by using scanning electron microscopy. A second critical aspect of this study was to provide transgene expression and enzyme activity evidence via western blots, tissue blot assays, and spectrophotometric assays. In addition, these data may be correlated to the phenotype data in order to better understand the effects of altering guard cell content of malate on stomata.

MATERIALS AND METHODS

Vector Construct

This research investigated Arabidopsis plants with guard cell specific NADP-ME expression via the KAT2 promoter (Pilot et al., 2001) or constitutive expression via the 35S promoter (Odell et al., 1985). Pooja Thakur cloned the KAT2 promoter to insert into the pMP535 vector and generate transgenic plants with guard cell specific NADP-ME expression (Thakur, 2006). Christine Notis utilized a pEG100 vector with a 35S promoter to generate transgenic Arabidopsis plants with constitutive NADP-ME expression. Both vectors contained the maize Me1 gene, 1733bp (Rothermel and Nelson, 1989), with a C-terminal penta-histidine (his) residue tag, and the portion of the gene encoding the chloroplast transit peptide was removed (Thakur, 2006). The maize ME gene was chosen because of its previously-observed effects on stomatal phenotype when constitutively expressed in tobacco (Laporte et al., 2002). The enzyme was his-tagged to allow for detection via western blot. The KAT2 promoter, 2258bp, and the maize ME gene were ligated into the pMP535 mini-binary vector (provided by Michael Prigge at the University of Michigan), 5405bp, which is based on the pCB302 vector (Xiang et al., 1999; Fig. 6). The maize ME gene was spliced into the pEG100 vector, which contained the 35S promoter, 9846bp (Earley et al., 2006), by a topoisomerase reaction (Fig. 7).

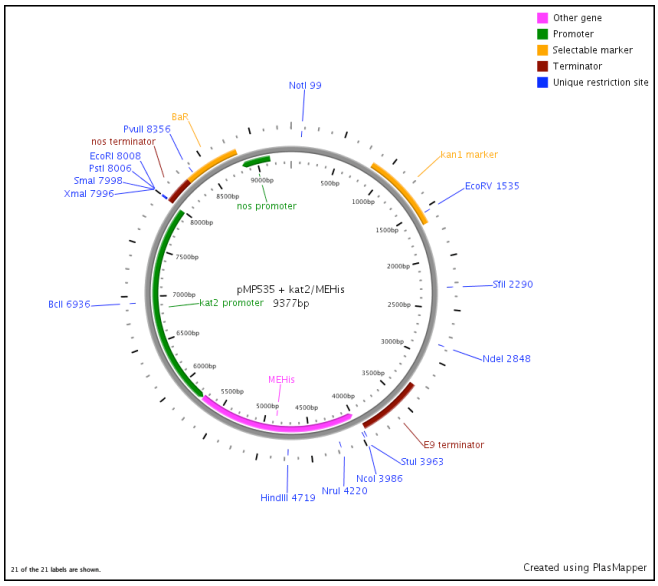

Figure 6. pMP535 vector construct with a KAT2 promoter and the maize ME gene (9377bp). The KAT2 promoter directs maize ME expression in Arabidopsis guard cells. The his tag allows for enzyme detection.

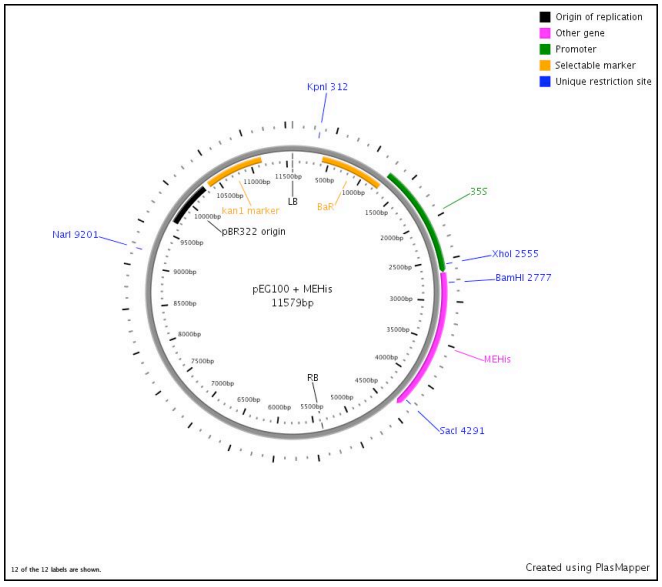

Figure 7. pEG100 vector construct with a 35S promoter and the maize ME gene (11579bp). The 35S promoter directs constitutive NADP-ME expression in Arabidopsis plants. The his tag allows for enzyme detection.

Plant Lines and Growth Conditions

The vector constructs were introduced into *Agrobacterium* by the freeze thaw technique (Hofgen and Willmitzer, 1988). The competent *Agrobacterium* were then used to transform healthy Arabidopsis (*Arabidopsis thaliana)* plants using the floral dip method (Clough and Bent, 1998). Successful transformants were screened for homozygous individuals, which were then utilized (Thakur, 2006). Unique transgenic lines resulted because NADP-ME inserted in different locations within the Arabidopsis genome during each transformation event. Empty-vector lines were also generated as a control against the transformation process. These plants were taken through the transformation process; however, the vector did not contain the maize ME gene.

Transgenic and wild-type Arabidopsis plants were grown in Conviron growth chambers (Winnipeg, Canada) between 48 to 70 d. The seeds were sown in a standard potting mix, watered daily, and fertilized once a week. The environmental parameters included 8-h-light at 20°C with an average PAR (photosynthetic active radiation) of 417 $\mu E\ m^{-2}\ sec^{-1}$ and 16-h-dark at 15°C with a relative humidity of 60%. The light source included four banks each of incandescent and fluorescent light bulbs.

Preliminary KAT2 Arabidopsis Morphological & Stomatal Count Analysis

SEM was employed to determine if the over-expression of NADP-ME has an effect on stomatal morphology and/or stomatal density. KAT2 plant lines were compared to wild-type Arabidopsis. Specimens were harvested 56-d after sowing from the first whorl of leaves (Fig. 8) and before the Arabidopsis bolting stage.

Figure 8. KAT2-transgenic line 1 Arabidopsis plant. Specimens were selected from the first whorl of leaves, as indicated by the perimeter of the circle.

Samples included wild-type and transgenic lines KAT2-1, KAT2-5, and KAT2-6, with n = 3 for each line. Samples were selected from consistently sized, mature, fully expanded leaves and were cut 1 cm in from the tip of the leaf. The specimens were fixed in 1.6% paraformaldehyde and 2.5% glutaraldehyde in 0.1 M sodium cacodylate buffer (pH 7.2) at 4°C overnight. Next, the specimens were washed thrice for 5 min each in 0.1 M sodium cacodylate buffer, before post-fixation in 0.5 to 1% osmium tetroxide for 30 min. Two washes in distilled water were followed by a 10-min wash in 50% ethanol, then a 10-min wash in an ascending, graded-ethanol series to three 5-min washes in 100% ethanol. The specimens were exposed to two 5-min washes in HMDS, and degassed overnight in the hood. The samples were then placed in a vacuum desiccator for approximately 2 hr and then stored at room temperature. Using colloidal graphite, the leaves were then mounted with the abaxial surface up on the stubs, sputter-coated with gold, and examined with a scanning electron microscope (Amray 1820I, KLA Tencor, San Jose, CA, USA) at an accelerating voltage of 5 kV. Specimens were examined under various magnifications with a working distance of 13 mm.

KAT2 and 35S Arabidopsis Stomatal Count Analysis

To determine if over-expressing NADP-ME elevates stomatal density among KAT2 and 35S plants relative to wild-type Arabidopsis, several SEM analyses were performed. A stomatal count analysis of fully expanded, older leaves was done. Specimens were harvested 62-d after sowing from the second whorl of leaves (Fig. 9) and before the bolting stage.

Figure 9. 35S-transgenic line 3 Arabidopsis plant. Specimens were selected from the second whorl of leaves, as indicated by the perimeter of the circle.

Samples included wild-type, KAT2, and 35S plants. For the KAT2 plants, transgenic lines KAT2-1, KAT2-2, KAT2-3, KAT2-5, and KAT2-6 and empty vector lines KAT2-A and KAT2-D were harvested, with n = 5 for each line. For the 35S plants, 35S-1, 35S-2, 35S-3, 35S-4 and empty vector lines 35S-A, 35S-B were analyzed, with n = 5 for each line. Samples were selected from consistently sized, mature, fully expanded leaves and were cut under preservative with a 0.5 cm leaf punch from either side of the central vein. The specimens were fixed in 2.5% paraformaldehyde and 5% glutaraldehyde in 0.05 M phosphate buffer (pH 7.0) at 4°C overnight on an orbital shaker. Next, the specimens were washed thrice for 5 min each in 0.05 M phosphate buffer, followed by a 30 min

wash in 50%, and then one 30 min wash at each concentration, in an ascending, graded-ethanol series to three 30 min washes in 100% ethanol. The specimens were exposed to two washes of 5 min each in HMDS and degassed overnight in the hood. The specimens were prepared for SEM viewing according to the above directions. Specimens were examined under various magnifications at an accelerating voltage of 5 kV and with a working distance of 18 mm. The number of stomata was determined within a 400 x 250 μm box at 300X. Stomata that were on the top and left boundaries were included, while stomata on the right and bottom boundaries were excluded from the counts. Micrographs were taken at random locations on the leaf.

KAT2 and 35S Arabidopsis Stomatal Count Using an Alternative Preservative

A second stomatal count analysis of fully expanded, older leaves was performed under different preservative conditions. Specimens were harvested 48-d after sowing from the second whorl of leaves (Fig. 9) and before the Arabidopsis bolting stage. Samples included wild-type, KAT2, and 35S plants. For the KAT2 plants, transgenic lines KAT2-1, KAT2-2, KAT2-3, KAT2-5, and KAT2-6 and empty vector lines KAT2-A and KAT2-D, with n = 6 for wild-type and n = 4 for transgenic line samples were analyzed. For the 35S plants, 35S-1, 35S-2, 35S-3, 35S-4 and empty vector lines 35S-A, 35S-B, were analyzed, with n = 4 for each line. Samples were selected from consistently sized, mature, fully expanded leaves and were removed using a 0.5 cm diameter leaf punch, while submerged in 70% ethanol. The specimens were fixed in 70% ethanol. Next, the specimens were washed once for 5 min in 70% ethanol, followed by two 5 min washes in 100% ethanol. Then the specimens were exposed to one 5 min wash in HMDS and were degassed overnight in the hood. The samples were then placed in a vacuum desiccator

for approximately 2 hours and then stored at room temperature. The specimens were prepared for SEM and viewed according to the above directions.

KAT2 and 35S Arabidopsis Developmental Series Stomatal Count of Older Leaves

A third stomatal count analysis of fully expanded, younger leaves was performed to determine if an exaggerated effect exists among transgenic lines relative to wild-type Arabidopsis. In addition, to improve leaf-choice constancy, a developmental series was generated for each individual plant analyzed (Fig. 10). The developmental series included removing the plant from soil, submerging it in water to remove excess debris and to retard leaf desiccation, and cutting off and numbering each leaf in series, starting from the oldest to the youngest (Fig. 10). Samples were selected from the second whorl from the top, because leaves were relatively young and large enough for analysis (Fig. 11). Samples were selected within a leaf range, numbered 22-43, by choosing consistently sized, fully expanded leaves. Specimens were harvested 53-d after sowing and before the Arabidopsis bolting stage. Samples included wild-type, KAT2, and 35S plants. For the KAT2 plants, transgenic lines KAT2-1, KAT2-2, KAT2-3, KAT2-5, and KAT2-6 and empty vector line KAT2-A were analyzed, with n = 6 for wild-type and n = 4 for transgenic line samples. For the 35S plants, 35S-1, 35S-2, 35S-3, 35S-4 and empty vector line 35S-A were analyzed, with n = 4 for each line. Specimens were removed using a 0.5 cm diameter leaf punch, while submerged in 70% ethanol. The specimens were fixed in 70% ethanol. Next, the specimens were washed once for 5 min in 70% ethanol, followed by one 5 min wash in 100% ethanol. Then the specimens were exposed to one 5 min wash in HMDS and were degassed overnight in the hood. The specimens were prepared for SEM and viewed according to the above directions.

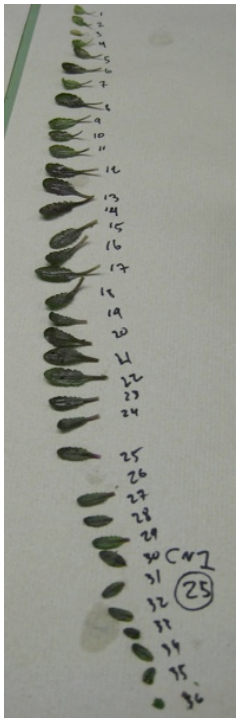

Figure 10. Leaf developmental series from 35S-transgenic line 1 Arabidopsis. Leaves were removed and numbered from the oldest to the youngest.

Figure 11. KAT2-transgenic line 6 Arabidopsis plant. Specimens were selected from the second whorl from the top, as indicated by the perimeter of the circle. Leaves were chosen within a leaf range of 22-43.

Statistical Analysis

A computer statistical software package, Systat 11 & 12, was employed to perform a statistical analysis of the stomatal count data. Since more than two independent populations were considered, ANOVA was used to determine if a statistically significant difference exists among transgenic and wild-type lines. If ANOVA detected a statistically significant difference, Dunnett's test was employed to perform a pair-wise comparison of each population's mean to wild-type in order to detect statistical significance. With this test, each transgenic line is compared to the control, the wild-type, thereby reducing the number of comparisons and increasing statistical power. All assumptions, including a normally distributed population and equal variance among populations, were confirmed for the ANOVA test.

The null hypothesis tested was H_o: Transgenic line stomatal count = Wild-type stomatal count, while the H_a: Transgenic line stomatal count > Wild-type stomatal count. A one-tail alternative hypothesis was posed because preliminary data indicated that over-expression of NADP-ME increased stomatal density. By looking only in one direction, statistical power was increased.

Detection of NADP-ME Transcript by RT-PCR

A Qiagen RNase easy plant minikit was used to detect the NADP-ME transcript via RT-PCR according to Thakur, 2006. KAT2 transgenic plant RT-PCR reactions were set up using 12.5 μL of 2X Access Quick RT-PCR master mix, 0.5 μL of 10pm/μL maize ME forward primer starting at 909bp (5'-TGACCCATCAGTTTGCTTGC- 3'), 0.5 μL of 10pm/μl maize ME reverse primer starting at 1603bp (5'-AATGCGAGGTTGGGTTTGAC-3'), 20 ng extracted RNA, and 0.2 μL AMV reverse

transcriptase. Autoclaved distilled water was added to bring the total volume to 25 μL. Amplification conditions were as follows: 48°C for 45 min, denaturation at 95°C for 2 min; 30 cycles at 95°C for 30 s, 55°C for 30 s, and 72°C for 30 s, followed by 72°C for 5 min for the final extension. PCR products were resolved on a 1% agarose gel to confirm the presence of the cDNA band.

35S transgenic plant RT-PCR reactions were set up by Christine Notis using 10 μL of 2X Access Quick RT-PCR master mix, 0.5 μL of 10pm/μL maize ME forward primer starting at 909bp (5'-TGACCCATCAGTTTGCTTGC-3'), 0.5 μL of 10pm/μl maize ME reverse primer starting at 1603bp (5'-AATGCGAGGTTGGGTTTGAC-3'), 10 ng extracted RNA, 0.2 μL AMV reverse transcriptase and 10.3 μL autoclaved distilled water. For the control reactions, which lacked reverse transcriptase, the above parameters were followed, but no AMV reverse transcriptase was added. Amplification conditions were as follows: 48°C for 45 min, denaturation at 94°C for 2 min; 32 cycles at 94°C for 15 s, 54°C for 1 min, and 72°C for 45 s, followed by 68°C for 7 min for the final extension. PCR products were resolved on a 1% agarose gel to confirm the presence of the cDNA band (Thakur, 2006).

Detection of NADP-ME by Immunoblotting Overview

A primary antibody directed against the his-tagged NADP-ME allowed for protein detection between transgenic KAT2 and 35S plants. Both whole leaf and guard cell protoplasts (GCPs) were homogenized to liberate NADP-ME. GCPs are plant cells lacking a cell wall and were isolated to confirm that the KAT2 promoter directs NADP-ME expression in guard cells. Extracted protein was quantified before analyzed via SDS-PAGE and western blot.

Guard Cell Protoplast Isolation

As described by Thakur 2006:

> Protoplast isolation was carried out using twenty fully expanded leaves from soil grown *Arabidopsis* transformants and wild type plants. The leaves were placed in approximately 100 mL of cold tap water after excision of the mid vein, and blended twice for 30 s in a Waring blender. The mixture was poured through a 200 μm Spectrum® nylon filter in an apparatus attached to an aspirator to remove broken mesophyll and epidermal cells. Any large green specks of mesophyll tissue were removed from the filter with forceps. All remaining peels were thoroughly rinsed with deionized water to remove the foam produced by the blending. All peels were scraped from the mesh into a flask containing 15ml of enzyme solution 1, which consists of 0.7% cellulysin cellulase, *Trichoderma viride*, 0.1% (w/v) PVP-40, 0.25% (w/v) bovine serum albumin, 0.5mM L-ascorbic acid, 0.1% cordycepin, and 0.0033% actinomycin D, all dissolved in 55% (v/v) basic solution and 45% (v/v) distilled water. This mixture of the peel in enzyme solution 1 was left in a shaking incubator at 27^{o} C with 140 rpm, for 40 min in dark. After 40 min, 37.5 mL of basic solution consisting of 5 mM MES hydrate, 0.5 mM $CaCl_2$, 0.5 mM $MgCl_2$, 10 μM KH_2PO_4, 0.5 mM L-ascorbic acid, 0.01% cordycepin, 0.0033% actinomycin D were added, and the osmolarity was adjusted to 550 mmol/kg by addition of D-sorbitol, pH 5.5 (using Tris

base) to a total volume of 300 mL. The mixture was then shaken under the same conditions for five minutes to provide an intermediate osmolarity between enzyme solutions 1 and 2 and prevent sudden plasmolysis of fragile guard cells. The digested peels were again poured through a fresh 200 μm Spectrum® nylon filter in the same apparatus as before, and rinsed with 10 to 15 mL of basic solution. The peels were scraped from the mesh with a spatula into a flask containing 15 mL of enzyme solution 2 composed of 1.3% (w/v) Onozuka RS cellulase, 0.0075% (w/v) Pectolyase Y-23, 0.25% (w/v) bovine serum albumin, 0.5 mM L-ascorbic acid, 0.1% cordycepin, and 0.0033% actinomycin D, pH 5.5. The flask was shaken at 20° C, 60 rpm, for 40 min in the dark and again at 20° C, 40 rpm, for 55 min in dark. The flask was swirled by hand for several seconds upon completion of the final digestion step in order to increase the liberation of guard cell protoplasts (GCPs) from the peels. The contents of the flask were poured through a 20 μm Spectrum® nylon filter in the same apparatus as before. The peels that remained on the filter were rinsed with 150 mL of basic solution as a final attempt to release GCPs. It is at this time that the GCPs in the filtrate are most readily viewed under a microscope. When a microscopic view reveals excessive debris or mesophyll presence, further filtration may be desired using a 10 μm Spectrum® nylon filter. The filtrate was collected in four 50-mL centrifuge tubes, and centrifuged for five minutes at 1000 x g. All but 1 to 1.5 mL of supernatant was removed using a pipette, as the pellet tends to be quite fragile. The pellet

in each tube was resuspended in 20 to 25 mL of basic solution followed by an identical centrifugation step. Again all but 1-1.5 mL of supernatant was removed. The 4-8 mL of the supernatant and pellet that remained in the five tubes was then combined and evenly distributed between 1.5 mL Eppendorf microcentrifuge tubes and centrifuged again for five minutes at 1000 x g. All but about 0.5 mL of supernatant was removed and the pellet was once again resuspended in basic solution so that it fits into one 1.5 mL Eppendorf microcentrifuge tube. This tube was centrifuged for five minutes at 1000 x g, all supernatant was removed, and the pellet was collected. (Thakur, 2006)

Crude Leaf and GCP Protein Extraction for SDS-PAGE and Western Blot

To enable NADP-ME quantification and detection, approximately 200 mg of whole leaf tissue and the yield of one GCP isolation (see above) were homogenized on ice in 1.5 mL and 150 μL extraction buffers (50 mM Hepes, 5 mM $MgCl_2$, and 1% PVPP), respectively. A protease inhibitor cocktail (Calbiochem) was added fresh to the extraction buffer in a 1:200 dilution. After liberating the protein, the supernatant was clarified by refrigerated centrifugation at 12,000 RPM for 2 min. The supernatant was stored at -20°C.

Protein Quantification

Once the protein was extracted, it was critical to determine the quantity of protein in the whole leaf and GCP extract for each sample to be used in SDS-PAGE. Bio-Rad protein assay dye reagent was used to determine the quantity of protein in each crude sample and Coomaise Brilliant Blue G-250, in 1:5 dilutions, was used to determine the

dilution factor required to bring each sample within range of the BSA (0.1mg/mL) standard curve. The protein samples were then measured at 570nm, and the readings were used to generate a BSA standard curve.

SDS-PAGE

Sodium dodecyl sulfate polyacrylamide gel electrophoresis (SDS-PAGE) was used to characterize and separate by molecular size whole leaf and GCP protein extractions. The advantage of a protein denaturing system includes separation of proteins based solely on size rather than other factors such as charge. Protein association with SDS beads induces it to unfold and results in a negatively charged primary protein structure. Electrophoresis separates SDS and protein complexes based on molecular size as they migrate towards the cathode.

Extracted protein from GCP and whole leaf samples were diluted in extraction buffer (5 mM $MgCl_2$, 50 mM Hepes, with 1% PVPP) to yield a final protein concentration of 10 µg/1 mL. The samples were then diluted 1:1 in Tris glycine SDS sample buffer (2X) containing 63 mM Tris-HCL, 10% Glycerol, 2% SDS, and 0.0025% bromophenol blue, pH 6.8 with 5% β-mercaptoethanol. To facilitate complete protein denaturation, the samples were incubated at 99°C for 15 min. Next, the heat-treated protein samples were loaded on a precast Novex 10%, 10-well Tris-glycine gel. The gel was loaded into an XCell Surelock gel box from Invitrogen. Separation took place using BioRad SDS trisglycine 10X buffer, with a working concentration of 1X running buffer at 95V for 1 hr. The positive control for the anti-his antibody included a purified malic enzyme with a his tag at both termini. The purified ME was diluted with extraction buffer to yield a final protein concentration of 2.26 mg/mL before diluting in sample buffer and heat-

treated as described above. Approximately 40 μL of protein was loaded. Proteins were visualized with Molecular Probes Coomassie Fluor Orange protein gel stain (Invitrogen) overnight on a rotary shaker.

Western Blot

SDS-PAGE, as described above, separated proteins based on their size and then NADP-ME was visualized by using a primary antibody directed against the his-tag. The proteins from the SDS-PAGE gel were electro-blotted to a nitrocellulose membrane using semi-dry transfer buffer (25 mM Tris, 150 mM glycine, and 10% methanol) at 125mAmps and 10V for 130 min. All subsequent steps were done while on an orbital shaker, unless otherwise noted. The membrane was then washed twice, 10 min each, in 30 mL 1X TBS buffer (10 mM Tris-Cl pH 7.5 and 150 mM NaCl). Then the membrane was washed in 30 mL blocking buffer (3% (w/v) BSA in TBS) for 1 hr to prevent non-specific primary antibody binding. The blot was then incubated in a TBS Tween/Triton solution (20 mM Tris-Cl pH 7.5, 500 mM NaCl, 0.05% (v/v) Tween 20, 0.2% (v/v) TritonX 100) twice for 10 min each wash, followed by a wash in 1X TBS for 10 min to remove remaining blocking buffer. Next, the membrane was incubated overnight with an α-His antibody (12.5 μL Anti-Penta-His Antibody, Qiagen, in 25 mL blocking buffer). The blot was washed twice, 10 min each wash, in TBS Tween/Triton and once in 1X TBS for 10 min. The blot was incubated with a secondary antibody (Goat α Mouse IgG Alkaline Phosphate Conjugate, Clontech) for 1 hr at room temperature. The membrane was washed 4 times, 10 min each, in TBS Tween/Triton to remove excess secondary antibody. The membrane was transferred into a 1-Step NBT/BCIP substrate solution and

exposed for 5 min, without shaking, to visualize the NADP-ME protein via a chemiluminescence reaction.

Determination of the SDS-PAGE and Western Blot Limit of Detection

Eric Rowley determined the limit of detection of the immunoblotting procedure by separating various concentrations of the purified NADP-ME control via SDS-PAGE (see above), followed by a western blot (see above).

NADP-ME Detection by Tissue Blot Assay

According to Wheeler et al., NADP-ME was extracted by homogenizing whole leaf samples (50-d-old) into extraction buffer containing 100 mM Tris-HCl, pH 7.5, 5 mM $MgCl_2$, 2 mM EDTA, 10% (v/v) glycerol, and 10 mM 2-mercaptoethanol. These reagents served to stabilize and maintain the enzyme's structure because the assay detects the reduction of NADP to NADPH (see Equation 1). Then samples were blotted onto a nitrocellulose membrane. Approximately 2 μL (2.1mg/mL) of the positive control (a purified malic enzyme with a his tag at both termini), 10 μL of the negative control (heat-treated wild-type protein extract), 10 μL of wild-type protein extract, and 10 μL of transgenic line protein extract were blotted onto the membrane. The nitrocellulose membrane was incubated in the tissue blot assay buffer (50 mM Tris-HCl, pH 7.5, 10 mM L-malate, 10 mM $MgCl_2$, 0.5 mM $NADP^+$, 35 mg/mL nitroblue tetrazolium (NBT), and 0.85 mg/mL phenazine methosulfate (PMS)) for 2 hr at room temperature. When NADP-ME is present and active, it catalyzes the reduction of NADP to NADPH (Equation 1). PMS serves as an electron acceptor, causing NADPH to be oxidized to NADP. While PMS is reduced, it is converted from a yellow compound to a colorless one. Oxidized PMS is regenerated when it is reduced by NBT, which is converted from a

yellow compound to a blue precipitate (Fig. 12). Hence, the formation of the blue precipitate indicates active NADP-ME (Wheeler et al., 2005).

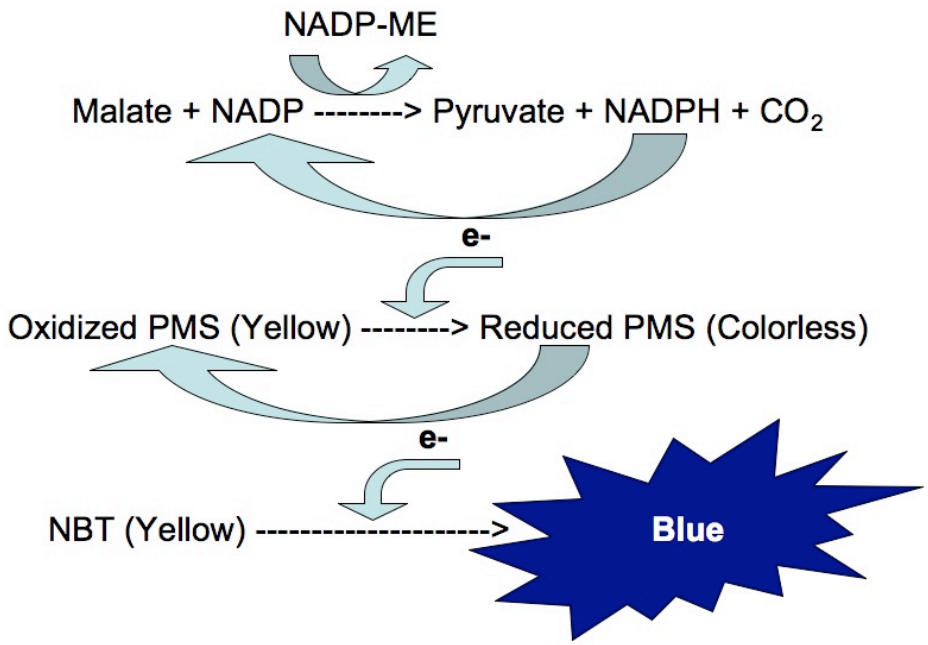

Figure 12. Chemical reactions catalyzed by the tissue blot assay buffer. NADP-ME's catalytic activity causes the reduction of NADP to NADPH. NADP is regenerated when PMS (phenozine methosulfate) acts as an electron acceptor and is reduced to a colorless substance. PMS is oxidized when it reduces NBT (nitroblue tetrazolium), causing the formation of a blue precipitant.

NADP-ME Specific Activity Measurement

A spectrophotometric analysis was utilized to measure the formation of NADPH by NADP-ME extracted from both transgenic KAT2 and 35S plants and wild-type Arabidopsis by providing the substrates, malate and $NADP^+$. Protein was extracted from 500 mg healthy transgenic and wild-type Arabidopsis plants. The enzyme was liberated in 1492.5 µL cold extraction buffer containing 50 mM Hepes (pH 8.0), 2.5 mM EDTA, 5 mM $MgCl_2$, 1% PVPP, 7.5 µL 1mM DTT, and 15 µL protease inhibitor Cocktail set III from Cal Biochem (1:1000 dilution) by using a glass homogenizer. The extract was

clarified by centrifugation and the supernatant was collected. An NADP assay cocktail was formulated to contain 895 µL assay buffer (50 mM Hepes (pH 8.0), 2.5 mM EDTA, and 4 mM malate with 40 µL 10 mM NADP and 5 µL DTT. This assay cocktail was utilized as a blank with the volume brought to 1 mL using the assay buffer versus the protein extract. The reaction was measured for 15 min once 20 µL of protein extract was added to the assay mix. This was necessary to limit background once the reaction was initiated with $MgCl_2$. The reaction was then measured at 340 nm because one product of the reaction catalyzed by NADP-ME is NADPH, which absorbs light maximally at 340 nm. The increased absorbance reading correlates with increased enzyme activity. After 15 min, the reaction was initiated with 40 µL 500 mM $MgCl_2$, with a final concentration of 20 mM in each 1 mL assay, and was measured at 340 nm for 15 min (Thakur, 2006). To determine specific activity, the extracted protein was quantified (see above) and the BSA calibration curve was used to determine the specific activity.

Statistical analysis was conducted using Systat 11 and 12. The null hypothesis tested was H_o: Transgenic line enzyme activity = Wild-type enzyme activity, while the H_a: Transgenic line enzyme activity > Wild-type enzyme activity. A one-tail alternative hypothesis was posed because it was expected that the activity of the enzyme would be elevated in the transgenic plants relative to wild-type. By looking in only one direction, statistical power was increased.

RESULTS

Preliminary KAT2 Arabidopsis Morphology & Stomatal Count Analysis

Comparison between wild-type and KAT2 transgenic Arabidopsis indicated no substantial morphological differences, although artifacts from the preservative process were evident. Fig. 13 indicates a pair of guard cells and a stomatal pore from wild-type Arabidopsis.

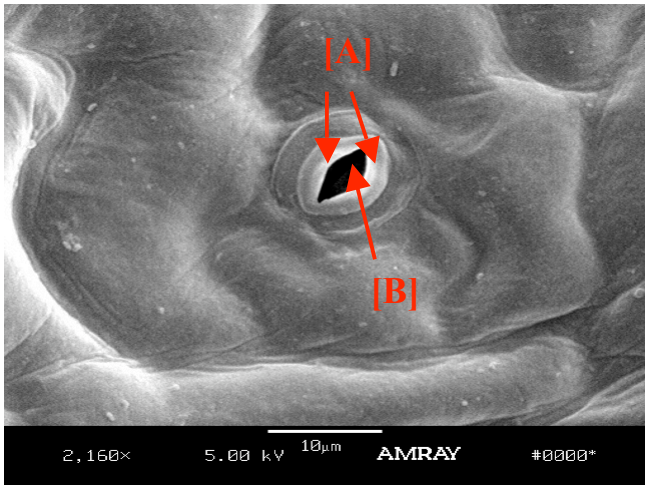

Figure 13. SEM micrograph of a wild-type Arabidopsis stomatal complex. Working Distance 13 mm. [A] indicates the pair of guard cells, and [B] open stomatal pore.

Direct comparisons between stomata from both the experimental and wild-type groups indicated no structural differences (Figs. 14, 15, 16), but the transgenic lines appeared to have preserved differently with respect to wild-type and each other. The transgenic lines indicated a gradient effect with respect to the intensity of preservative artifacts relative to wild-type. Preservative artifacts included tissue collapse and puckering, most likely due to differences in osmolarity between the tissue and the buffer. The micrographs indicated that KAT2-transgenic line 1 (Fig. 14) had the highest level of tissue stress around

stomatal complexes, followed by KAT2-transgenic line 6 (Fig. 15), and KAT2-transgenic line 5 (Fig. 16) appeared to have minimal evidence for preservative artifact.

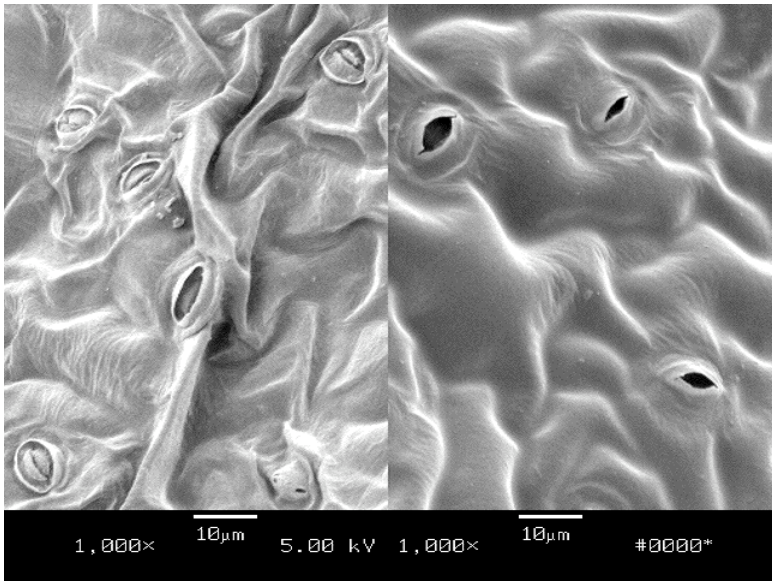

Figure 14. SEM micrograph of Arabidopsis stomatal complexes used for morphology analysis. Left Panel: KAT2-Transgenic Line 1. Right Panel: Wild-Type. Working Distance 13mm.

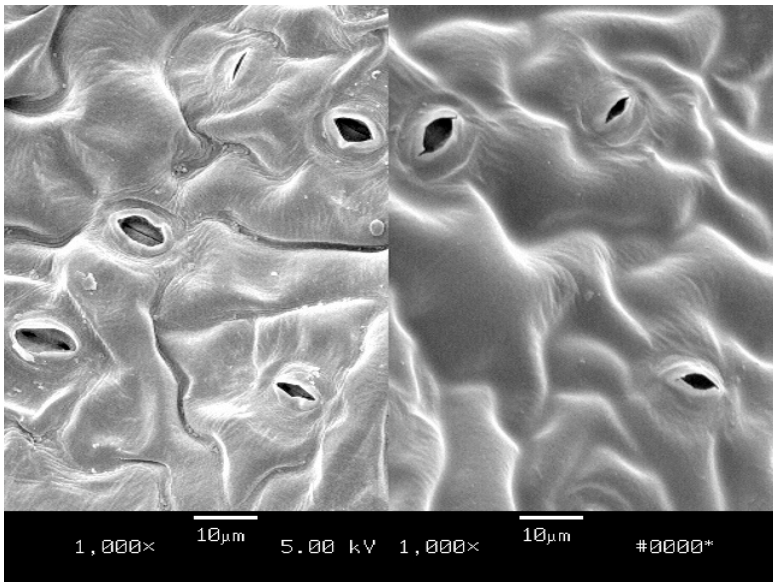

Figure 15. SEM micrograph of Arabidopsis stomatal complexes used for morphology analysis. Left Panel: KAT2-Transgenic Line 6. Right Panel: Wild-Type. Working Distance 13mm.

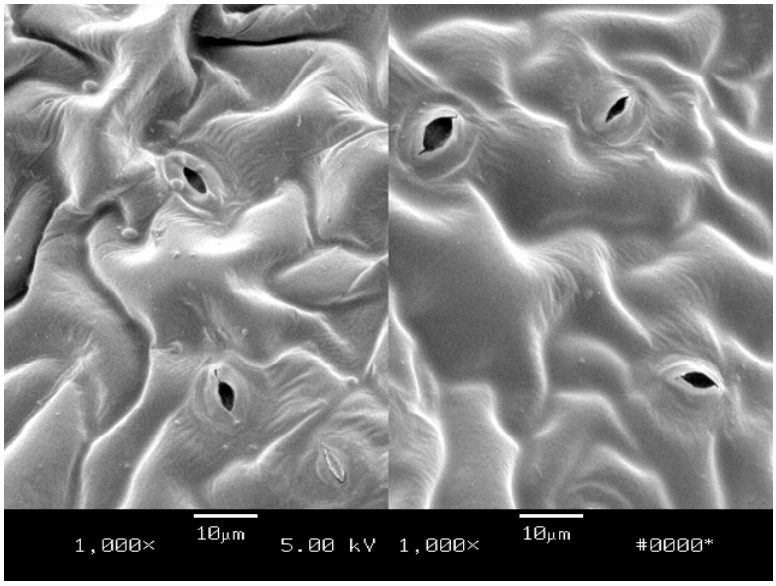

Figure 16. SEM micrograph of Arabidopsis stomatal complexes used for morphology analysis. Left Panel: KAT2-Transgenic Line 5. Right Panel: Wild-Type. Working Distance 13mm.

A preliminary stomatal count investigation indicated an elevated stomatal density in KAT2 transgenic lines relative to wild-type Arabidopsis (Fig. 17). These data suggested that a more thorough stomatal density investigation of the KAT2 transgenic plants was required.

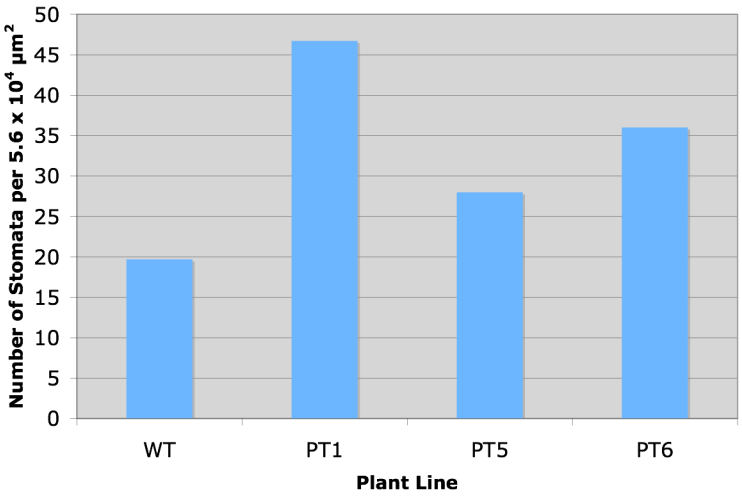

Figure 17. Preliminary scanning electron microscopy stomatal counts data on fully expanded wild-type and KAT2 transgenic Arabidopsis. These data indicate elevated stomatal densities in the transgenic lines (PT) relative to wild-type (WT), prompting further investigation. Plants were 56-d old, with all groups n = 1.

KAT2 and 35S Arabidopsis Stomatal Count Analysis

The combination of 2.5% paraformaldehyde and 5% glutaraldehyde in the 0.05 M phosphate buffer (pH 7.0) preservative appeared to have been ineffective in maintaining the plant tissue (Fig. 18). For an accurate stomatal count, it was imperative to have minimal preservative artifacts and a relatively planar surface. None of these specimens could be included in the stomatal count analysis.

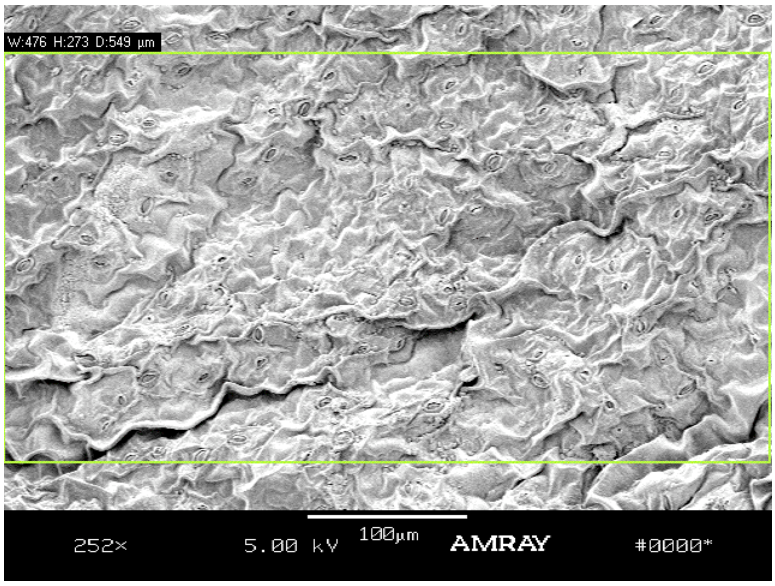

Figure 18. SEM micrograph of wild-type Arabidopsis stomatal complexes. This combination of preservative did not maintain the integrity well enough for stomatal counts. Working Distance 18 mm.

KAT2 and 35S Arabidopsis Stomatal Count of Older Leaves Using an Alternative Preservative & Statistical Analysis

A stomatal count analysis of fully expanded, older leaves was performed to determine if an exaggerated effect exists between transgenic KAT2 (Fig. 19) and 35S (Fig. 20) plant lines relative to wild-type Arabidopsis (Fig. 21). It was hypothesized that over-expressing NADP-ME in Arabidopsis guard cells would elevate stomatal density. For the KAT2 transgenic plants, empty vector KAT2-lines A and C and KAT2-transgenic line 2 indicated little difference in stomatal density relative to the wild-type (Fig. 22). However, transgenic lines KAT2-1, KAT2-3, KAT2-5, and KAT2-6 indicated elevated stomatal densities relative to the wild-type (Fig. 22). To assess whether statistical differences existed among the transgenic lines and wild-type, ANOVA was performed and its assumptions were confirmed.

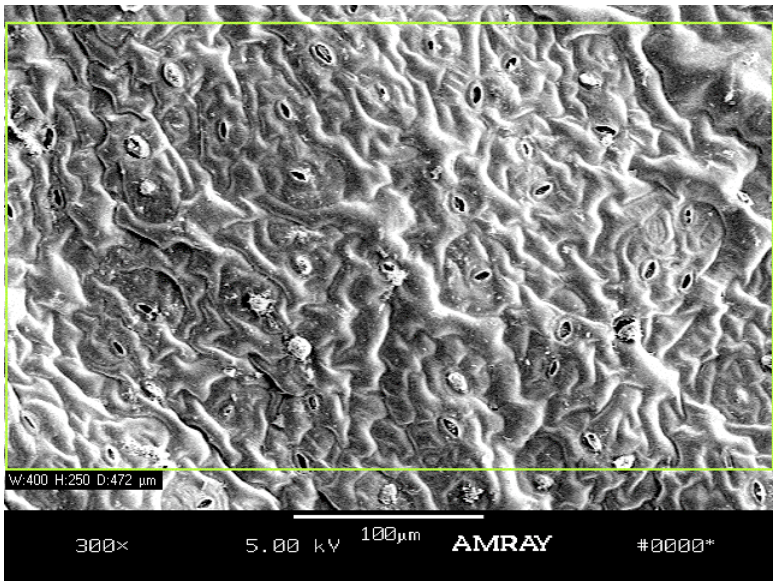

Figure 19. Stomatal count SEM micrograph of KAT2-transgenic line 1 Arabidopsis. The number of stomata were determined within a 400 x 250 µm box at 300X. Working Distance 18 mm.

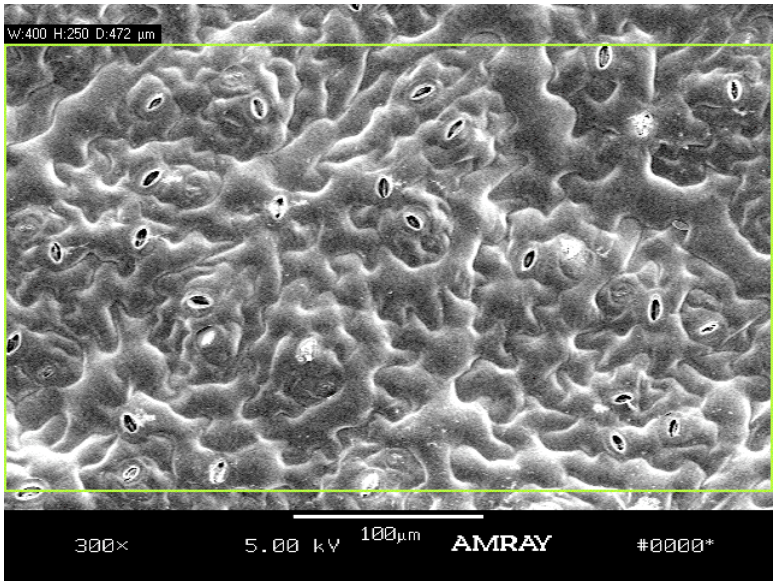

Figure 20. Stomatal count SEM micrograph of 35S-transgenic line 3 Arabidopsis. The number of stomata were determined within a 400 x 250 µm box at 300X. Working Distance 18 mm.

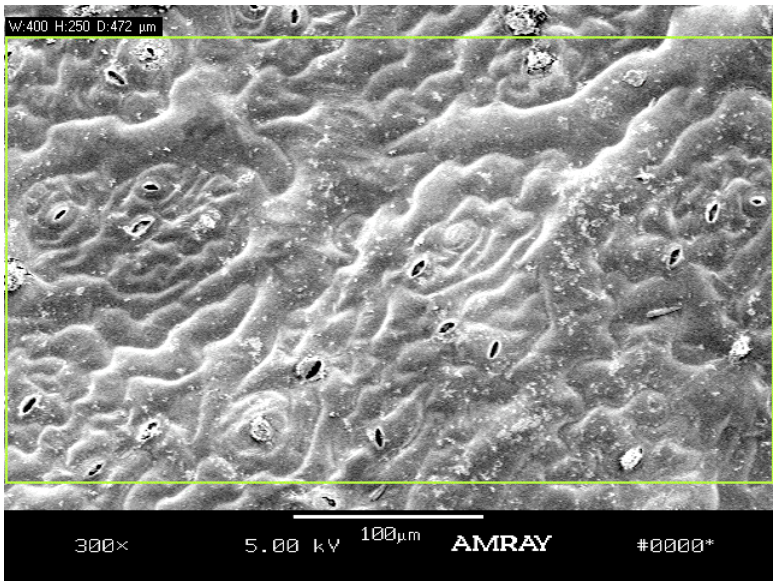

Figure 21. Stomatal count SEM micrograph of wild-type Arabidopsis. The number of stomata were determined within a 400 x 250 µm box at 300X. Working Distance 18 mm.

A scatter plot of the data indicated a consistent and a reasonable distribution of the data (Fig. 23). To meet the first assumption, random samples within the defined

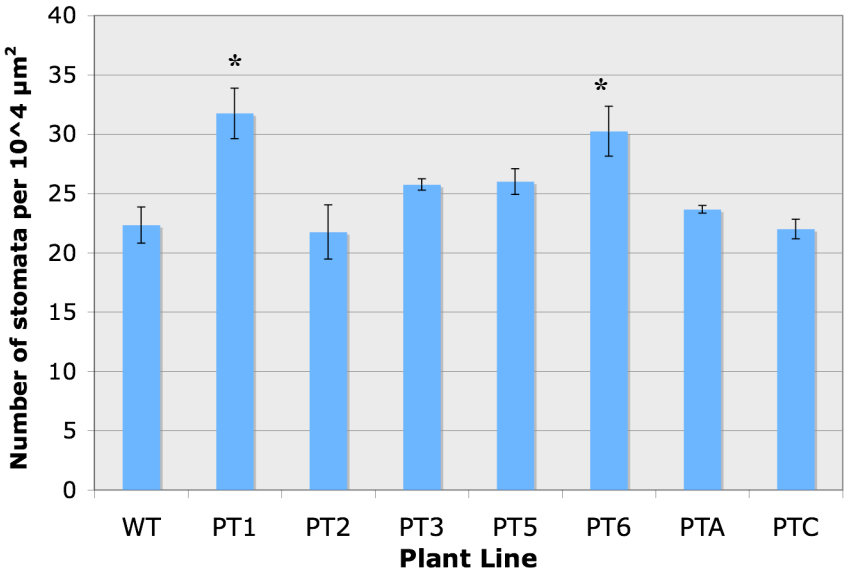

Figure 22. Number of stomata per 10^5 µm^2 for older, KAT2-transgenic lines (PT) and wild-type Arabidopsis leaves. This indicates PT 1 & 6 were statistically significant relative to wild-type. Specimens were approximately 50-d-old. All groups n=4, except for wild-type n=6 and PTA n = 3. PTA and PTC are empty vector lines. Standard error is reported.

parameters were harvested. The populations indicated a reasonably normal distribution, therefore meeting the second assumption for ANOVA (Fig. 24). The populations indicated relatively equal variances, hence meeting the third assumption for ANOVA (Fig. 24).

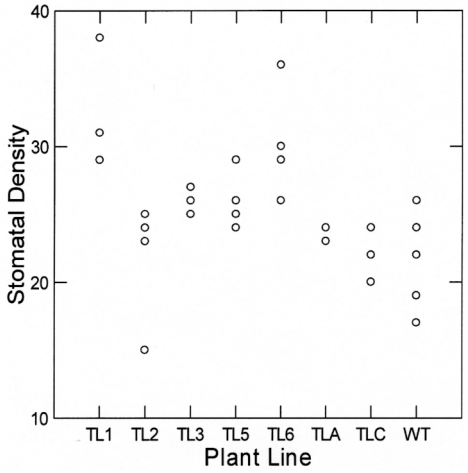

Figure 23. KAT2 Arabidopsis scatter plot of stomatal count data for older, KAT2 leafs. WT = Wild-type, TL = Transgenic line.

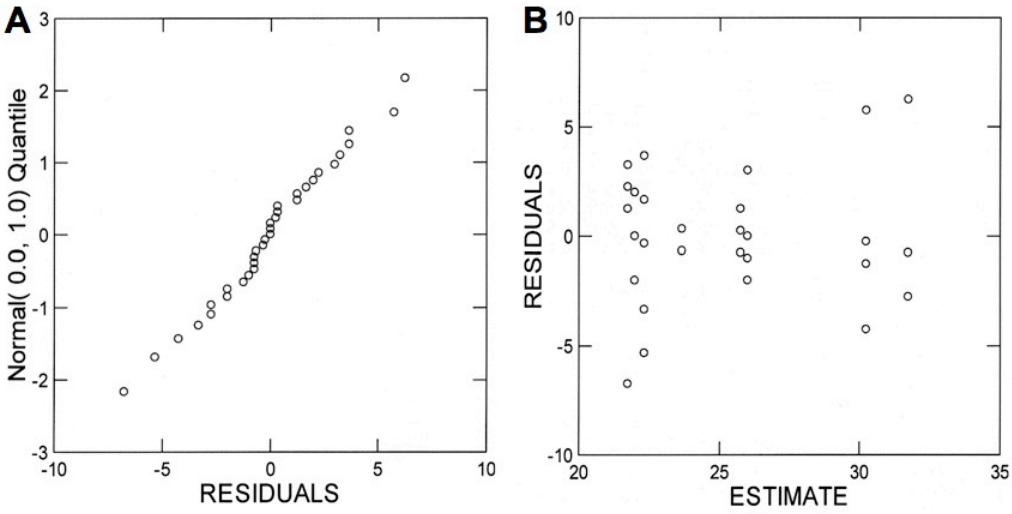

Figure 24. Confirmation for ANOVA assumptions of older, KAT2 leaf stomatal counts. A, Probability plot of the stomatal count data form all KAT2-transgenic lines and wild-type Arabidopsis populations. This indicated a relatively normal population distribution. B, Plot assessed variance among KAT2 transgenic lines and wild-type Arabidopsis populations. This indicated that the populations had relatively equal variances.

With the assumptions confirmed, the ANOVA output was considered robust, with n = 33. Figure 25 presents the results of ANOVA, which indicated that the calculated $p < \alpha = 0.05$, therefore the H_o is rejected ($p < 0.001$). ANOVA indicated that there was a statistical difference among the groups, but a pair-wise comparison was necessary to determine which lines had a statistically significant difference relative to wild-type.

Analysis of Variance

Source	Type III SS	df	Mean Squares	F-ratio	p-value
LINE$	421.96970	7	60.28139	5.68692	0.00052
Error	265.00000	25	10.60000		

Figure 25. ANOVA output for KAT2-transgenic and wild-type older leaf stomatal counts. The H_o was rejected ($p < 0.001$), indicating that the stomatal density elevation is statistically significant.

Dunnett's pair-wise comparison test indicated which lines exhibit a statistically significant difference relative to the wild-type (Fig. 26). The wild-type was set as the control and significance was detected in one direction, i.e. greater than 22.33 stomata / 100,000 μm^2. The stomatal counts for transgenic line 1 ($p < 0.001$) and transgenic line 6 ($p < 0.01$) were statistically significant relative to the wild-type. As a result, the alternative hypothesis (H_a: Transgenic stomatal count > Wild-type stomatal count) was not rejected for lines KAT2-1 and KAT2-6. The null hypothesis (H_o: Transgenic stomatal count = Wild-type stomatal count) was not rejected for all other lines. Older, fully expanded KAT2 leaves indicated an elevated stomatal density relative to wild-type Arabidopsis.

▼Hypothesis Tests

Post Hoc Test of COUNT
Using least squares means.
Dunnett Test with Control = WT
Using model MSE of 10.60000 with 25 df.

Dunnett Test(Greater than Control)			
LINE$(i)	LINE$(j)	Difference	p-value
TL1	WT	9.41667	0.00047
TL2	WT	-0.58333	0.49996
TL3	WT	3.41667	0.23980
TL5	WT	3.66667	0.20235
TL6	WT	7.91667	0.00283
TLA	WT	1.33333	0.49617
TLC	WT	-0.33333	0.50000

Figure 26. Dunnett's pair wise comparison test results for older, KAT2-transgenic and wild-type Arabidopsis leaves. Stomatal counts for KAT2-transgenic line 1 ($p < 0.001$) and KAT2-transgenic line 6 ($p < 0.01$) were significantly different relative to wild-type.

Stomatal counts also included the 35S plants, which constitutively overexpress NADP-ME, in order to determine the effect on stomatal density. For the 35S transgenic plants, empty vector lines A and C and transgenic line 4 indicated little difference in stomatal density relative to the wild-type (Fig. 27). However, transgenic lines 35S-1, 35S-2, and 35S-3 indicated elevated stomatal densities relative to the wild-type (Fig. 27). To assess whether statistical differences existed among the transgenic lines and wild-type, ANOVA was performed and its assumptions were confirmed. A scatter plot of the data indicated a consistent and a reasonable distribution of the data (Fig. 28). To meet the first assumption, random samples within the defined parameters were harvested. The populations indicated a reasonably normal distribution, therefore meeting the second assumption for ANOVA (Fig. 29). The populations indicated relatively equal variances, hence meeting the third assumption for ANOVA (Fig. 29).

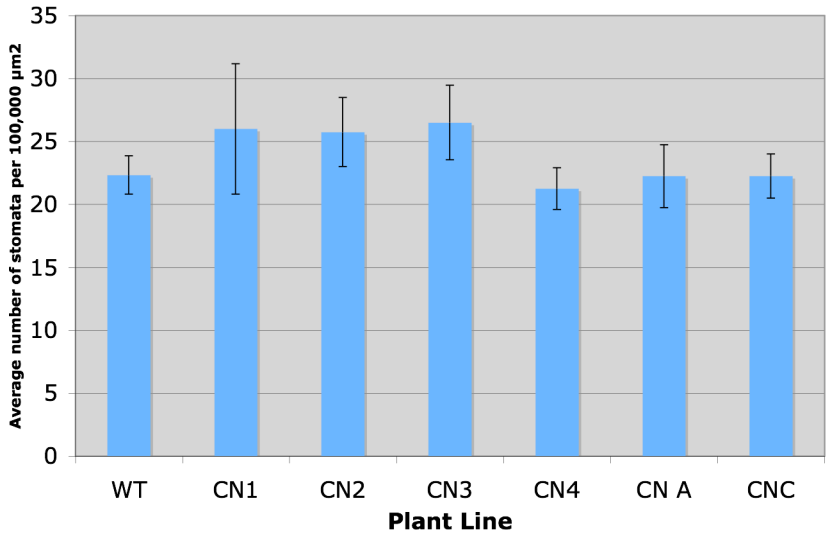

Figure 27. Number of stomata per 10^5 µm^2 for older, 35S-transgenic lines (CN) and wild-type Arabidopsis leaves. This indicates that none of the transgenic lines were statistically significant relative to wild-type. Specimens were approximately 50-d-old. All groups n=4, except for wild-type, n=6. CN A and CNC are empty vector lines. Standard error is reported.

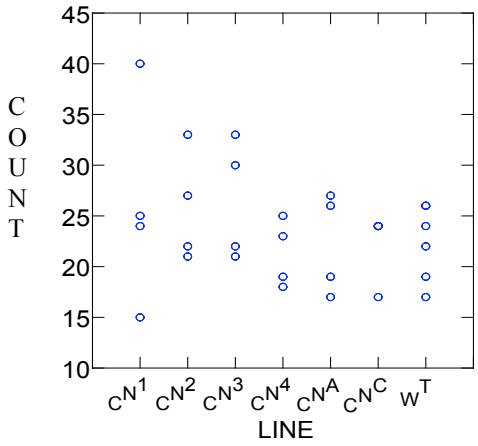

Figure 28. 35S Arabidopsis scatter plot of stomatal count data for older leaves. WT = Wild-type, CN = Transgenic line.

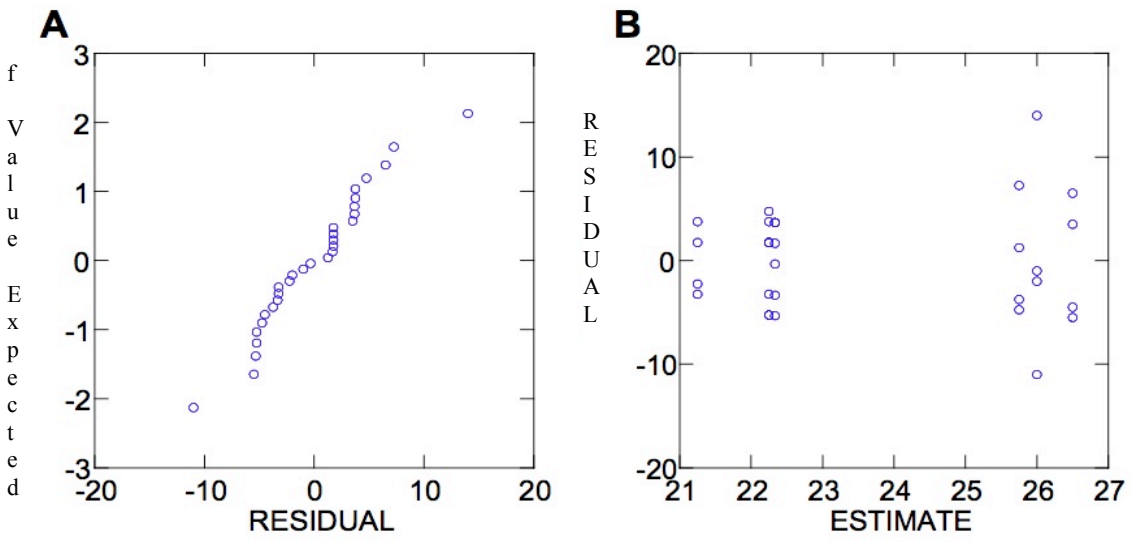

Figure 29. Confirmation for ANOVA assumptions of older, 35S leaf stomatal counts. A, Probability plot of the stomatal count data form all 35S-transgenic lines and wild-type Arabidopsis populations. This indicated a relatively normal population distribution. B, Plot assessed variance among 35S-transgenic lines and wild-type Arabidopsis populations. This indicated that the populations had relatively equal variances.

With the assumptions confirmed, the ANOVA output was considered robust, with n = 30. Figure 30 presents the results of ANOVA, which indicated that the calculated $p > \alpha = 0.05$; therefore, the H_o was not rejected. ANOVA indicated that there was not a statistical difference among the groups. A pair-wise comparison was not necessary to determine which lines had a statistically significant difference relative to wild-type. Therefore, the null hypothesis (H_o: Transgenic stomatal count = Wild-type stomatal count) was not rejected for all lines. Older, fully expanded 35S leaves did not indicate an elevated stomatal density relative to wild-type Arabidopsis.

Source	Sum-of-Squares	df	Mean-Square	F-ratio	P
LINE$	121.333	6	20.222	0.636	0.700
Error	731.333	23	31.797		

Figure 30. ANOVA output for 35S transgenic and wild-type, older leaf stomatal counts. The H_o was not rejected ($p > 0.05$), indicating that stomatal density differences were not statistically significant.

KAT2 and 35S Arabidopsis Developmental Series Stomatal Count of Younger Leaves & Statistical Analysis

A stomatal count analysis of fully expanded, younger leaves was performed to determine if an exaggerated effect exists between transgenic KAT2 and 35S plant lines relative to wild-type Arabidopsis. It was hypothesized that over-expressing NADP-ME in Arabidopsis guard cells would elevate stomatal density. For the KAT2 transgenic plants, all transgenic and empty vector lines indicated little difference in stomatal density relative to the wild-type (Fig. 31). To assess whether statistical differences existed among the transgenic lines and wild-type, ANOVA was performed and its assumptions were confirmed. A scatter plot of the data indicated a consistent and reasonable distribution of the data (Fig. 32). To meet the first assumption, random samples within the defined parameters were harvested. The populations indicated a reasonably normal distribution, therefore meeting the second assumption for ANOVA (Fig. 33). The populations indicated relatively equal variances, hence meeting the third assumption for ANOVA (Fig. 33).

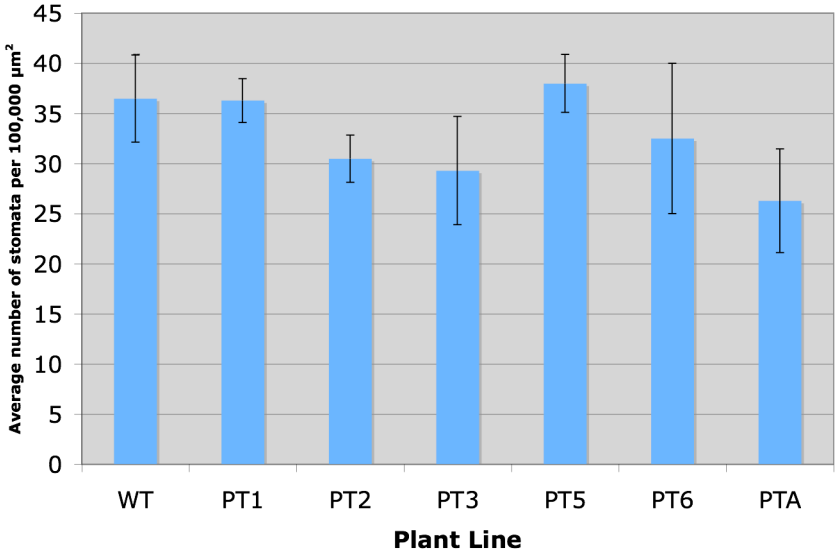

Figure 31. Number of stomata per 10^5 µm^2 for younger, KAT2-transgenic lines (PT) and wild-type Arabidopsis leaves. This indicates none of the transgenic lines were statistically significant relative to wild-type. Specimens were approximately 53-d-old. All groups n=4, except for wild-type n=6, PT1 n=3, PT5 n=3, PT6 n=2, and PTA n=3. PTA is an empty vector lines. Standard error is reported.

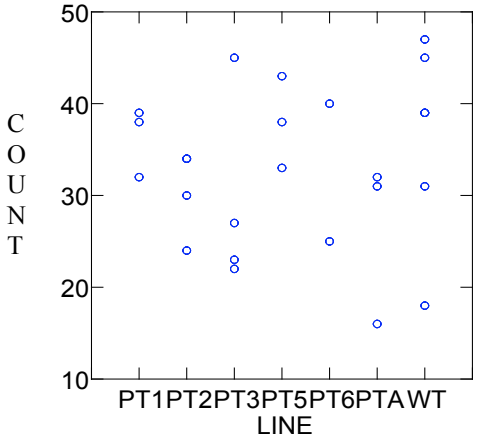

Figure 32. KAT2 Arabidopsis scatter plot of younger leaf, stomatal count data. WT = Wild-type, PT = Transgenic line.

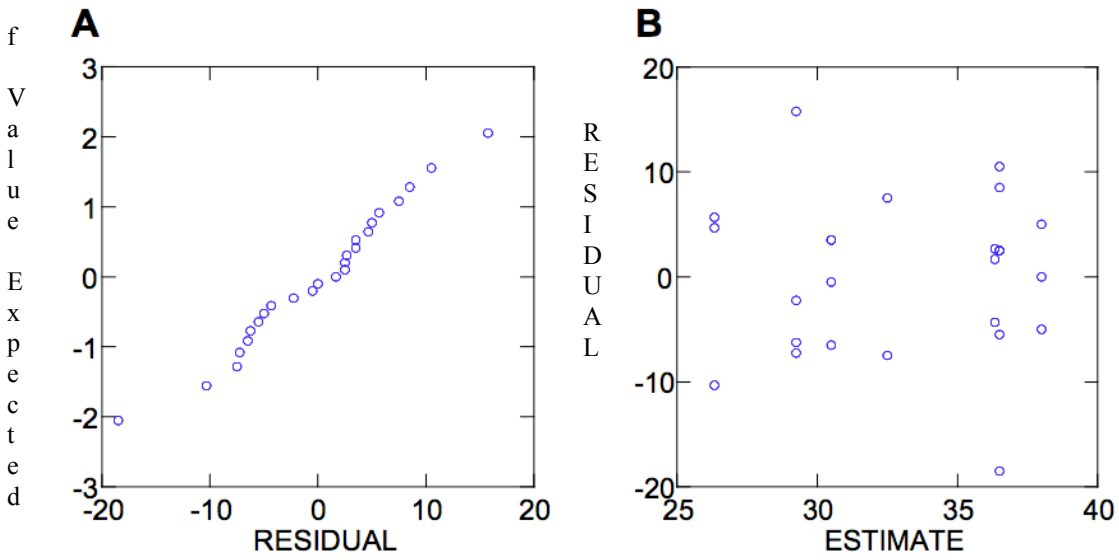

Figure 33. Confirmation for ANOVA assumptions for younger, KAT2 leaf stomatal counts. A, Probability plot of the stomatal count data form all KAT2-transgenic lines and wild-type Arabidopsis populations. This indicated a relatively normal population distribution. B, Plot assessed variance among KAT2-transgenic lines and wild-type Arabidopsis populations. This indicated that the

With the assumptions confirmed, the ANOVA output was considered robust, with n = 25. Figure 34 presents the results of ANOVA, which indicated that the calculated $p > \alpha = 0.05$; therefore, the H_o is not rejected. ANOVA indicated that there was not a statistical difference among the groups. A pair-wise comparison was not necessary to determine which lines had a statistically significant difference relative to wild-type. Therefore, the null hypothesis (H_o: Transgenic stomatal count = Wild-type stomatal count) was not rejected for all lines. Old, fully expanded KAT2 leaves did not indicate an elevated stomatal density relative to wild-type Arabidopsis.

Source	Sum-of-Squares	df	Mean-Square	F-ratio	P
LINE$	396.917	6	66.153	0.895	0.520
Error	1331.083	18	73.949		

Figure 34. ANOVA output for KAT2-transgenic and wild-type, younger leaf stomatal counts. The H_o was not rejected ($p > 0.05$), indicating that stomatal density differences were not statistically significant.

Stomatal counts also included the 35S plants, which constitutively over-express NADP-ME, in order to determine the effect on stomatal density under such a condition. For the 35S transgenic plants, empty vector line A and transgenic lines 35S-1 and 35S-2 indicated little difference in stomatal density relative to the wild-type (Fig. 35). However, transgenic lines 35S-3 and 35S-4 indicated elevated stomatal densities relative to the wild-type (Fig. 35). To assess whether statistical differences existed among the transgenic lines and wild-type, ANOVA was performed and its assumptions were confirmed. A scatter plot of the data indicated a consistent and reasonable distribution of the data (Fig. 36). To meet the first assumption, random samples within the defined parameters were harvested. The populations indicated a reasonably normal distribution, therefore meeting the second assumption for ANOVA (Fig. 37). The populations indicated relatively equal variances, hence meeting the third assumption for ANOVA (Fig. 37).

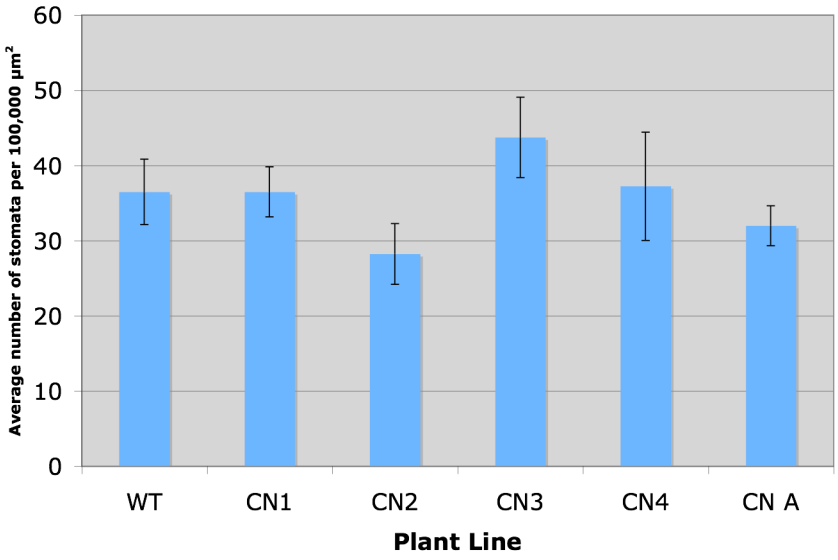

Figure 35. Number of stomata per 10^5 µm^2 for younger, 35S-transgenic lines (CN) and wild-type Arabidopsis leaves. This indicates none of the transgenic lines were statistically significant relative to wild-type. Specimens were approximately 53-d-old. All groups n=4, except for wild-type, n=6. CN A is an empty vector lines. Standard error is reported.

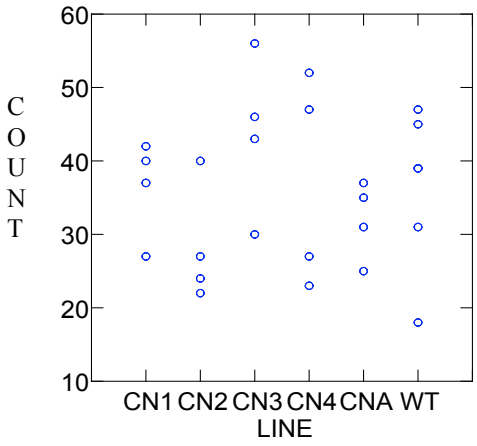

Figure 36. 35S Arabidopsis scatter plot of younger leaves, stomatal count data. WT = Wild-type, CN = Transgenic line.

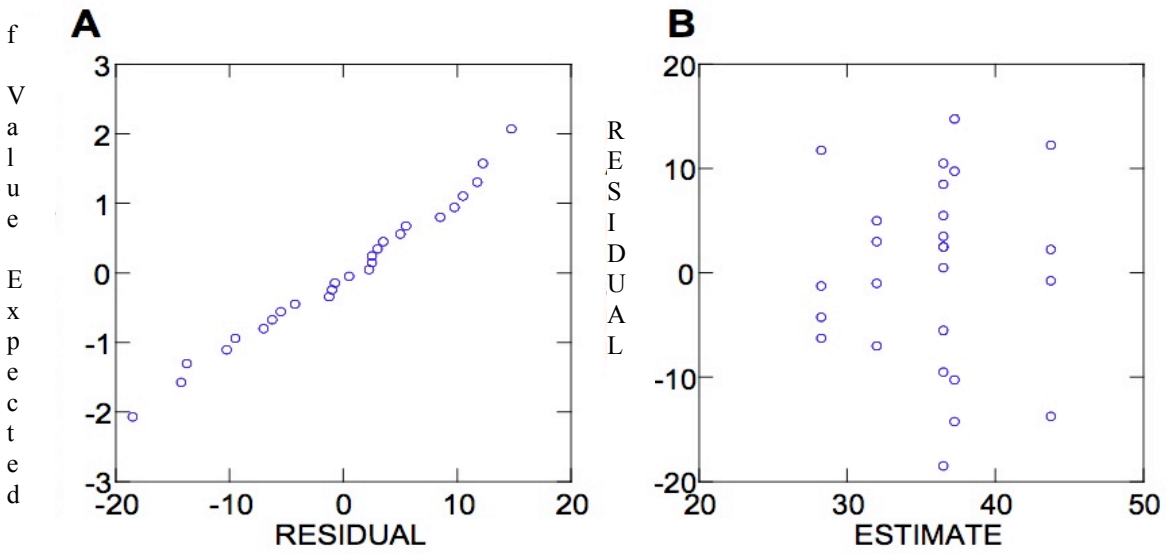

Figure 37. Confirmation for ANOVA assumptions of younger, 35S leaf stomatal counts. A, Probability plot of the stomatal count data form all 35S-transgenic lines and wild-type Arabidopsis populations. This indicated a relatively normal population distribution. B, Plot assessed variance among 35S-transgenic lines and wild-type Arabidopsis populations. This indicated that the populations

With the assumptions confirmed, the ANOVA output was considered robust, with n = 26. Figure 38 presents the results of ANOVA, which indicated that the calculated $p > \alpha = 0.05$; therefore, the H_o was not rejected. ANOVA indicated that there was not a statistical difference among the groups. A pair-wise comparison was not necessary to determine which lines had a statistically significant difference relative to wild-type. Therefore, the null hypothesis (H_o: Transgenic stomatal count = Wild-type stomatal count) was not rejected for all lines. Young, fully expanded 35S leaves did not indicate an elevated stomatal density relative to wild-type Arabidopsis.

Source	Sum-of-Squares	df	Mean-Square	F-ratio	P
LINE$	551.865	5	110.373	1.134	0.375
Error	1946.750	20	97.338		

Figure 38. ANOVA output for 35S-transgenic and wild-type, younger leaves stomatal counts. The H_o was not rejected ($p > 0.05$), indicating that stomatal density differences were not statistically significant.

Detection of NADP-ME Transcript by RT-PCR

RNA was extracted from wild-type, KAT2 and 35S transgenic Arabidopsis and subjected to a RT-PCR in order to detect the NADP-ME gene transcript. Analysis of KAT2 Arabidopsis whole leaf RNA extractions indicated that the gene, specifically a 700bp portion, was successfully transcribed in transgenic lines KAT2-1, KAT2-2, KAT2-3, and KAT2-6 (Fig. 39, Lanes 2 to 5). However, the gene transcript was not present in the wild-type (negative control) RNA extraction (Fig. 39, Lane 1).

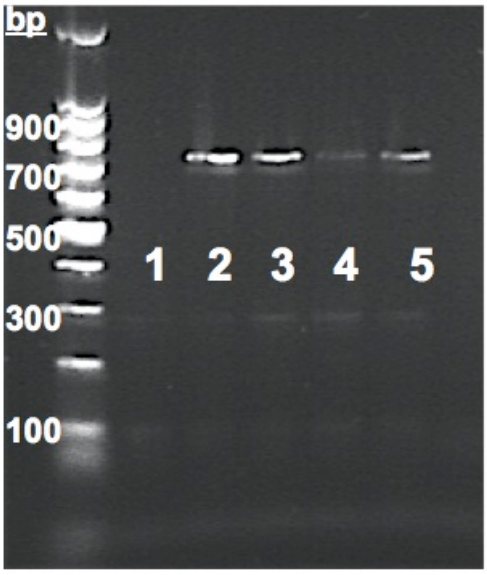

Figure 39. RT-PCR of KAT2 transgenic and wild-type Arabidopsis RNA extractions. The NADP-ME gene transcript was detected in all transgenic whole leaf samples at approximately 700 bp (Lanes 2 to 5). The transcript was not detected in the negative control, wild-type Arabidopsis (Lane 1). Lane 1, wild-type (negative control). Lane 2, transgenic line 1. Lane 3, transgenic line 2. Lane 4, transgenic line 3. Lane 5, transgenic line 6.

Analysis of 35S Arabidopsis whole leaf RNA extractions indicated that the gene was successfully transcribed in transgenic lines 35S-1, 35S-3, and 35S-4 (Fig. 40A, Lanes 2 to 4). However, the gene transcript was not present in the wild-type (negative control) RNA extraction (Fig. 40A, Lane 1). An additional negative control, to control for DNA contamination, with no reverse transcriptase was included, which indicated a lack of genomic DNA contamination of the RNA preparation (Fig. 40B, Lanes 1 to 4).

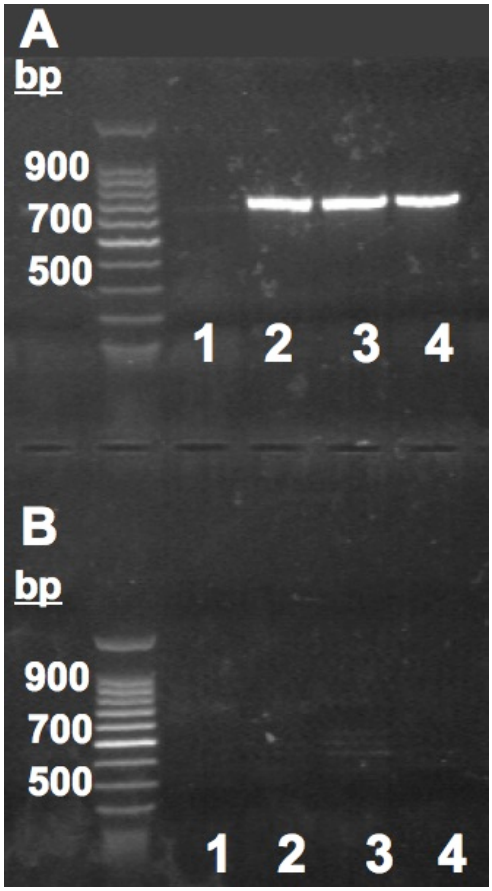

Figure 40. RT-PCR of 35S transgenic and wild-type Arabidopsis RNA extractions. A, The NADP-ME gene transcript was detected in all transgenic whole leaf samples at approximately 700 bp (Lanes 2 to 4). The transcript was not detected in the negative control, wild-type Arabidopsis (Lane 1). Lane 1, wild-type (negative control). Lane 2, transgenic line 1. Lane 3, transgenic line 3. Lane 4, transgenic line 4. B, No reverse transcriptase control. The transcript was not detected in either wild-type or transgenic Arabidopsis RNA extractions (Lanes 1 to 4). Lane 1, wild-type. Lane 2, transgenic line 1. Lane 3, transgenic line 3. Lane 4, transgenic line 4.

Protein Quantification

After extracting protein from wild-type and transgenic 35S and KAT2 Arabidopsis, the total protein concentration was determined by using a BSA standard curve with a serial dilution of 0.1to 2.5 mg/mL BSA (Figure 41). This was used to determine the quantity of protein loaded for SDS-PAGE.

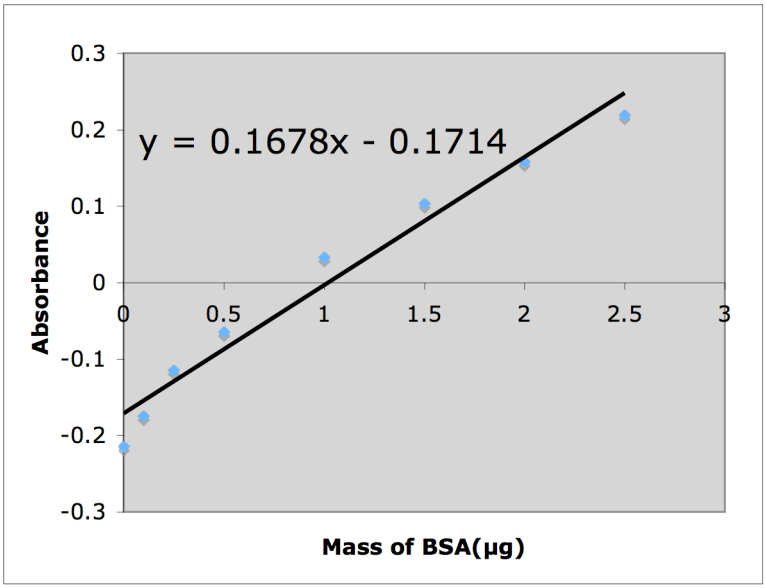

Figure 41. BSA standard curve generated by a serial dilution of 0.1 to 2.5 mg/mL BSA. The y-axis represents the absorbance at 450nm, while the x-axis indicates the protein concentration.

SDS-PAGE

A primary antibody directed against the his-tagged NADP-ME was utilized to provide transgene expression evidence. SDS-PAGE was first used to characterize whole leaf and GCP protein extractions based on molecular size. The positive control was a purified 72 kDa NADP-ME with a C-terminal his tag and an N-terminal his- thioredoxin tag (109 amino acids, Novagen, Madison, WI). The negative controls included both whole leaf and GCP extractions from wild-type Arabidopsis. SDS-PAGE separated GCP protein extractions from KAT2 transgenic lines 3 and 6 and empty vector line A and whole leaf

protein extractions from KAT2-transgenic line 3 and 35S-transgenic line 1 (Fig. 42). NADP-ME is approximately 62 kDa (Edward et al., 1992). The positive control was detected at approximately 72 kDa (Fig. Z). Lanes 2 (negative control: wild-type Arabidopsis GCP), 3 (KAT2 transgenic line 3 GCP), 4 (KAT2 empty vector line A GCP), and 5 (KAT2 transgenic line 6 GCP) indicated no protein within the expected size for NADP-ME(Fig. Z). The whole leaf extracts indicated, in lanes 6 (negative control: wild-type Arabidopsis whole leaf), 7 (KAT2 transgenic line 3 whole leaf) and 8 (35S transgenic line 1 whole leaf), the presence of a high concentration of protein at approximately 55 kDa. It was not NADP-ME because bands appeared in the negative control, lane 6, and the transgenic lines, lanes 7 to 8 (Fig. 42). Instead, that distinctive band was the smaller subunit of RuBisCo, with a molecular weight of 55 kDa. RuBisCo saturated the whole leaf samples, while the GCP samples did not have RuBisCo.

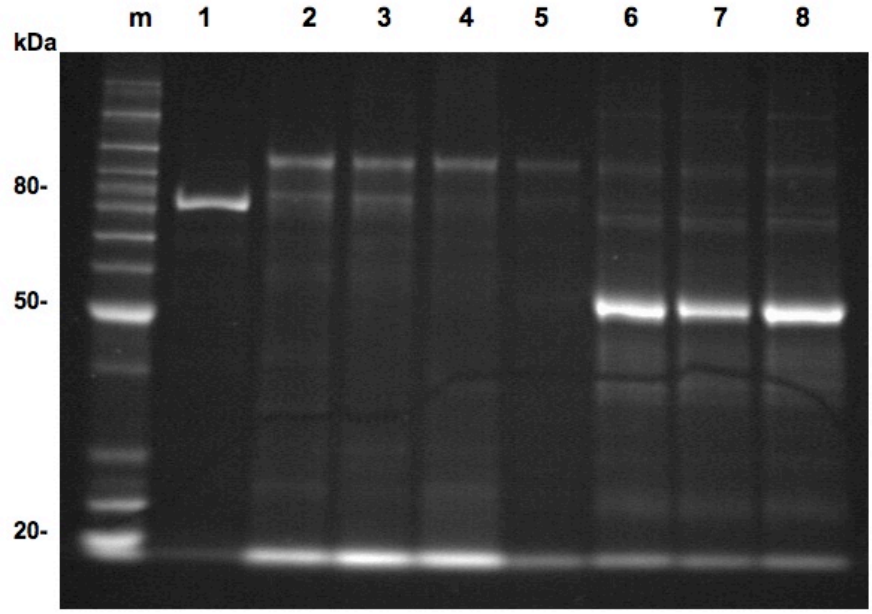

Figure 42. Transgenic KAT2 and 35S whole leaf and GCP protein extractions analyzed by a Coomassie Fluor Orange stained SDS-PAGE protein gel. m, Protein marker. Lane 1, 2.25 µg positive control: 72 kDA purified NADP-ME with a C-terminal his tag and a N-terminal his-trx tag. Lane 2, 10 µg negative control: wild-type Arabidopsis GCP. Lane 3, 10 µg KAT2 transgenic line 3 GCP. Lane 4, 10 µg KAT2 empty vector line A GCP. Lane 5, 10 µg KAT2 transgenic line 6 GCP. Lane 6, 10 µg negative control: wild-type Arabidopsis whole leaf. Lane 7, 10 µg KAT2 transgenic line 3 whole leaf. Lane 8, 10 µg 35S transgenic line 1 whole leaf. NADP-ME is approximately 62 kDa.

Immunoblotting/Western Blot

After separating the proteins by SDS-PAGE, they were electro-blotted onto a nitrocellulose membrane, which was then exposed to the anti-his primary antibody. The positive control was a purified 72 kDa, NADP-ME with a C-terminal his tag and a N-terminal his-trx tag. The negative controls included both whole leaf and GCP extractions from wild-type Arabidopsis. Samples analyzed included GCP protein extractions from KAT2 transgenic lines 3 and 6 and empty vector line A and whole leaf protein extractions from KAT2 transgenic line 3 and 35S transgenic line 1 (Fig. 43). NADP-ME is approximately 62 kDa. The positive control was detected at approximately 72 kDa

(Fig. 43). Lanes 2 to 5 (Fig. 43) indicated no protein within the expected size for NADP-ME. The primary antibody detected a protein at approximately 55 kDa for the whole leaf protein extracts, lanes 6 to 8 (Fig. 43). This band, however, did not represent NADP-ME since this band also appeared in the negative control, lane 6 (Fig. 43). Instead, this distinctive band may be the smaller subunit of RuBisCo, which has a molecular weight of 55 kDa. Thus, the primary antibody appeared to cross-react with RuBisCo (Fig. 43, Lanes 6 to 8).

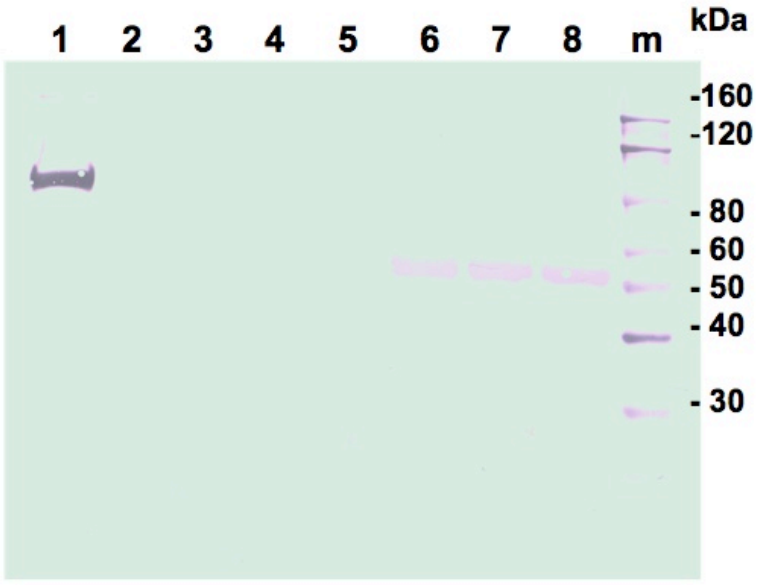

Figure 43. Western blot of KAT2 and 35S extracted proteins. Transgenic KAT2 and 35S whole leaf (from 34-d-old plants) and GCP (from 70-d-old plants) protein extractions analyzed by a western blot. Lane 1, positive control: 72 kDA purified NADP-ME with a C-terminal his tag and a N-terminal his-trx tag. Lane 2, negative control: wild-type Arabidopsis GCP. Lane 3, KAT2 transgenic line 3 GCP. Lane 4, KAT2 empty vector line A GCP. Lane 5, KAT2 transgenic line 6 GCP. Lane 6, positive control: wild-type Arabidopsis whole leaf. Lane 7, KAT2 transgenic line 3 whole leaf. Lane 8, 35S transgenic line 1 whole leaf. m, his-tagged protein marker. NADP-ME is approximately 62 kDa. The primary antibody cross-reacted with the smaller subunit of RuBisCo, which is 55 kDa, lanes 6, 7, and 8.

Determination of the SDS-PAGE and Western Blot Limit of Detection

The limit of detection of the immunoblotting procedure was determined to be less than 250 ng of the purified NADP-ME control, since this quantity was not visible on the stained SDS-PAGE gel, whereas it was visible on the stained western blot (Fig. 44).

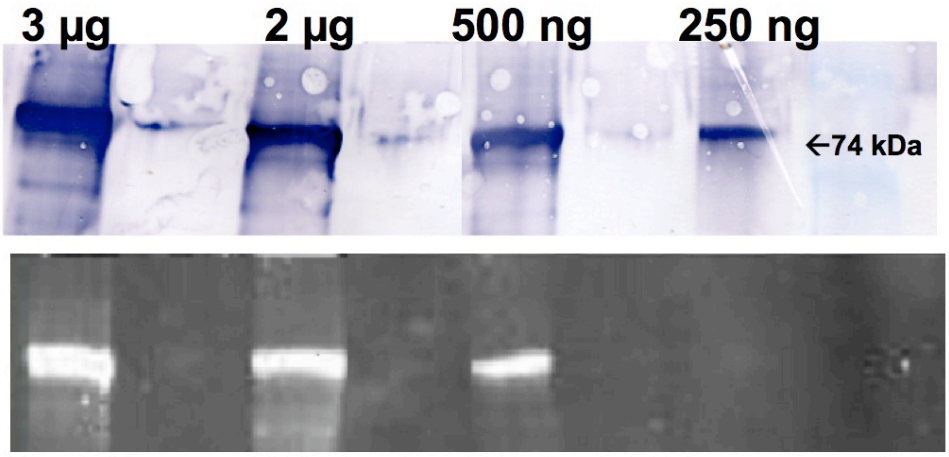

Figure 44. Limit of detection for the immunobloting procedure. Western blot (top) and stained SDS-PAGE gel (bottom) indicating a concentration gradient of purified His-tagged NADP-ME control to determine limit of detection. Limit of detection of the system was determined to be less than 250 ng, although this quantity was not visible on the gel, it was on the blot.

NADP-ME Detection by Tissue Blot Assay

The NADP-ME tissue blot assay revealed the presence of active NADP-ME in transgenic and wild-type Arabidopsis whole leaf protein extractions. The positive control, purified NADP-ME, (Fig. 45, b) indicated active enzyme because it catalyzed the formation of blue precipitate (reduced NBT). The wild-type contained NADP-ME activity, as expected, because this enzyme is extensively found throughout nature (Fig. 45, a). The transgenic lines also indicated enzymatic activity (Fig. 45, c to e). The negative control, boiled wild-type, had no visualization (not shown).

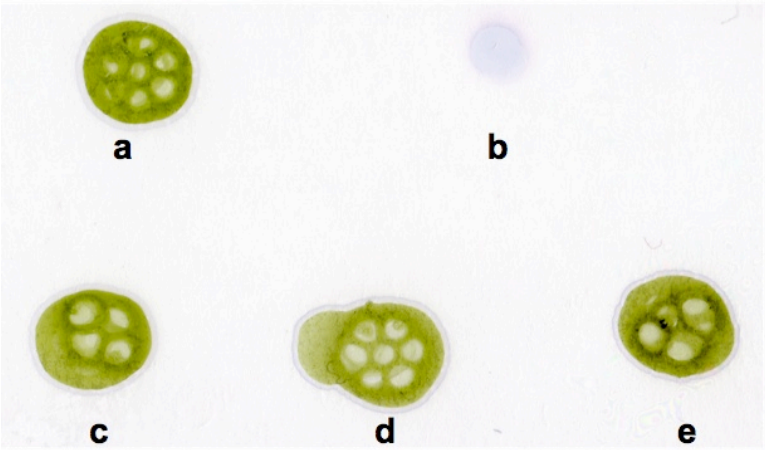

Figure 45. NADP-ME tissue assay blot of wild-type and transgenic Arabidopsis whole leaf protein extractions. a to e, whole leaf wild-type, purified NADP-ME (positive control), whole leaf 35S transgenic line 3, whole leaf KAT2 transgenic line 1, and whole leaf KAT2 transgenic line 6. Not shown: negative control, boiled WT protein extraction with no NADP-ME activity. All blotted samples indicated active NADP-ME, shown by the formation of blue precipitant (reduced NBT). Wild-type indicated NADP-ME activity, as expected because this enzyme is ubiquitous (Fig. 1, a).

NADP-ME Specific Activity Measurement

The specific activity of NADP-ME extracted from KAT2 and 35S transgenic plants were measured against their BSA standard curves, Fig. 46 and Fig. 47, respectively, after determining the total protein concentration in the extracts.

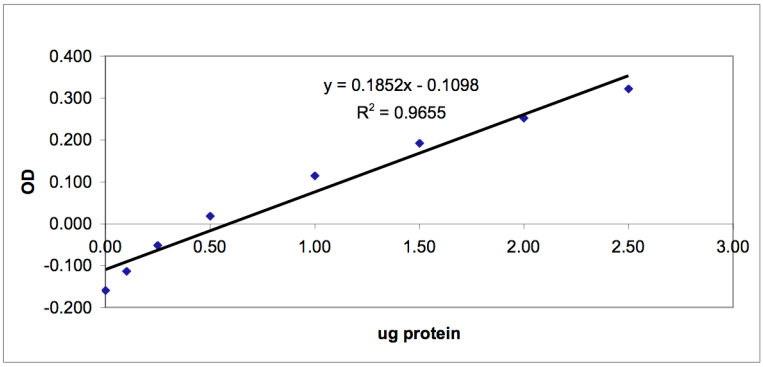

Figure 46. BSA standard curve for KAT2 transgenic plant extracted protein for spectrophotometric assay. The curve was generated by a serial dilution of 0.1 to 2.5 mg/mL BSA. The y-axis represents the absorbance at 450nm, while the x-axis indicates the protein amount.

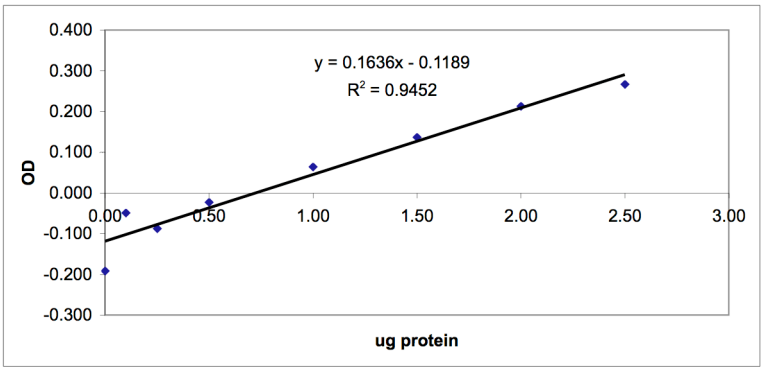

Figure 47. BSA standard curve for 35S transgenic plant extracted protein for spectrophotometric assay. The curve was generated by a serial dilution of 0.1-2.5 mg/mL BSA. The y-axis represents the absorbance at 450nm, while the x-axis indicates the protein amount.

The equations from the BSA standard curves were used to determine the total protein in the extract. The specific activity of ME was calculated by utilizing the following equation:

$((\Delta A_{340}{}^{ME}/min) - (\Delta A_{340}{}^{bckgnd}/min)) * (1mol\ NADPH/6270\ OD.1.cm) * (1\ cm/1) * (1*10^{-3}\ L/1) * (1mL/x\ mg\ protein) * (1/0.02\ mL) * (10^{6}\ \mu mol/1\ mol)$

where the $1*10^{-3}$ L/1 is the assay volume 1 mL and the 1/0.02 mL is the 20 µL sample used in the assay mix.

For the KAT2 transgenic plants, all transgenic and empty vector lines indicated little difference in enzyme activity relative to wild-type (Fig. 48). To assess whether statistical differences existed among the transgenic lines and wild-type, ANOVA was performed and its assumptions were confirmed. A scatter plot of the data indicated a consistent and reasonable distribution of the data (Fig. 49). To meet the first assumption, random samples were harvested. The populations indicated a reasonably normal distribution, therefore meeting the second assumption for ANOVA (Fig. 50). The populations

indicated relatively equal variances, hence meeting the third assumption for ANOVA (Fig. 50).

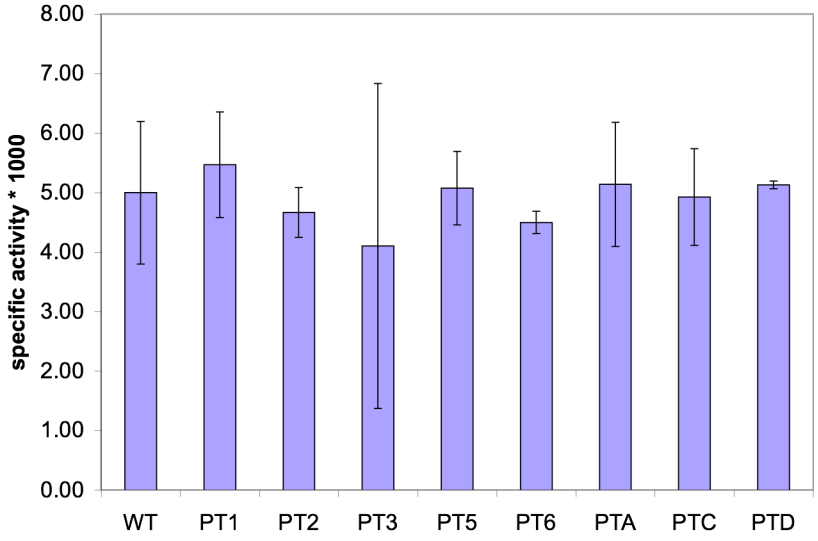

Figure 48. Enzyme activity in 16-d-old KAT2-transgenic and wild-type Arabidopsis. There was not a statistically significant difference in enzyme activity between transgenic and wild-type plants. Wild-type (WT), PT1-PT6 (KAT2-transgenic lines 1-6), PTA-PTD (KAT2-empty-vector lines A-D).). Standard error is reported and n=3 for each line except wild-type, n=2.

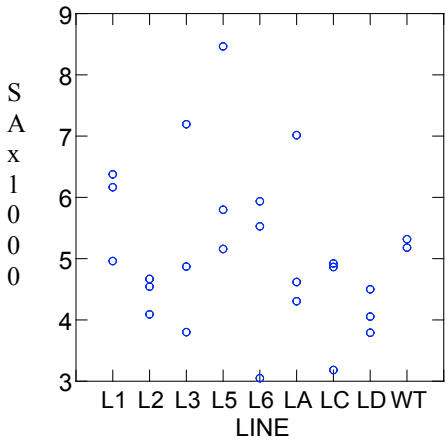

Figure 49. KAT2-transgenic Arabidopsis scatter plot of NADP-ME activity measurement data. Y-axis indicates enzyme specific activity x 1000. WT = Wild-type, L1-L6 = KAT2-Transgenic line, LA-LD = KAT2-Empty Vector Line.

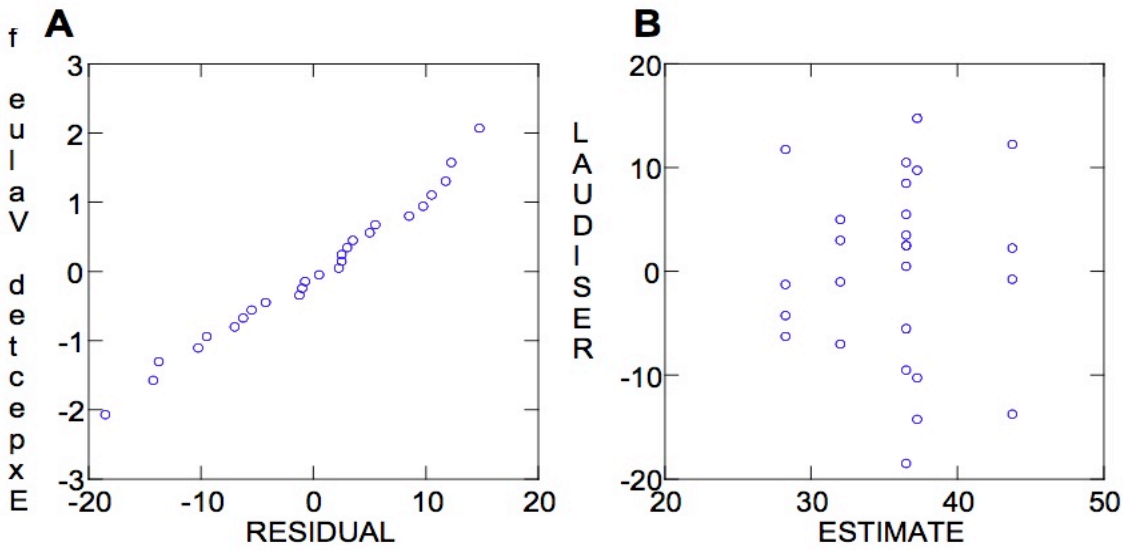

Figure 50. Confirmation of ANOVA assumptions for KAT2 enzyme activity. A, Probability plot of the enzyme activity data form all KAT2-transgenic lines and wild-type Arabidopsis populations. This indicated a relatively normal population distribution. B, Plot assessed variance among KAT2-transgenic lines and wild-type Arabidopsis populations. This indicated that the populations had

With the assumptions confirmed, the ANOVA output was considered robust, with n = 26. Figure 51 presents the results of ANOVA, which indicated that the calculated $p > \alpha = 0.05$; therefore, the H_o was not rejected. ANOVA indicated that there was not a statistical difference among the groups. A pair-wise comparison was not necessary to determine which lines had a statistically significant difference relative to wild-type. Therefore, the null hypothesis (H_o: Transgenic enzyme activity = Wild-type enzyme activity) was not rejected for all lines. KAT2 transgenic plants did not indicate a statistically significant elevation in NADP-ME activity relative to wild-type Arabidopsis.

Source	Sum-of-Squares	df	Mean-Square	F-ratio	P
LINE$	13.818	8	1.727	1.174	0.369
Error	25.019	17	1.472		

Figure 51. ANOVA output for the KAT2-transgenic and wild-type enzyme activity measurements. The H_o was not rejected ($p > 0.05$), indicating that enzyme activity differences were not statistically significant.

For the 35S transgenic plants, all transgenic and empty vector lines indicated elevated enzyme activity relative to wild-type (Fig.52). To assess whether statistical differences existed among the transgenic lines and wild-type, ANOVA was performed and its assumptions were confirmed. A scatter plot of the data indicated a consistent and reasonable distribution of the data (Fig. 53). To meet the first assumption, random samples were harvested. The populations indicated a reasonably normal distribution, therefore meeting the second assumption for ANOVA (Fig. 54). The populations indicated relatively equal variances, hence meeting the third assumption for ANOVA (Fig. 54).

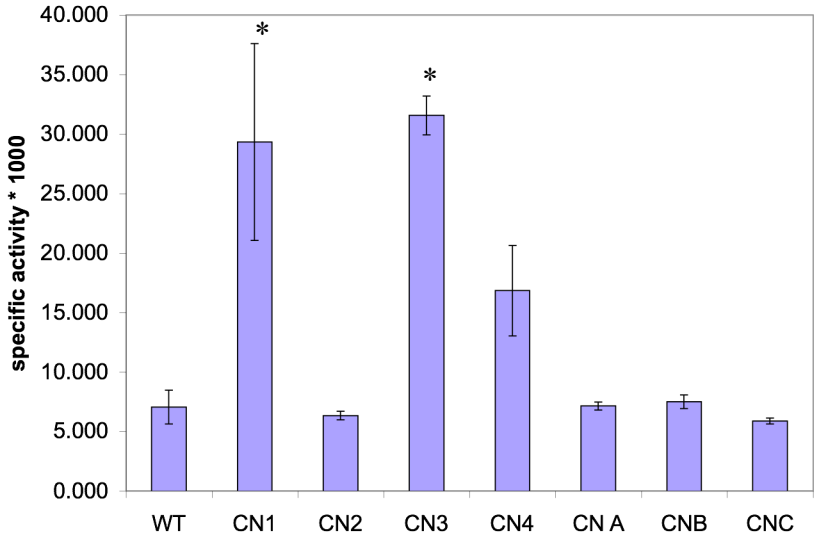

Figure 52. Enzyme activity in 29-d-old 35S-transgenic and wild-type Arabidopsis. There was a statistically significant difference among transgenic lines 1 and 3 relative to wild-type enzyme activity. Wild-type (WT), CN1-CN4 (35S-transgenic lines 1-4), CN A- CNC (35S-empty-vector lines A-C). Standard error is reported and n=2 for each line and wild-type.

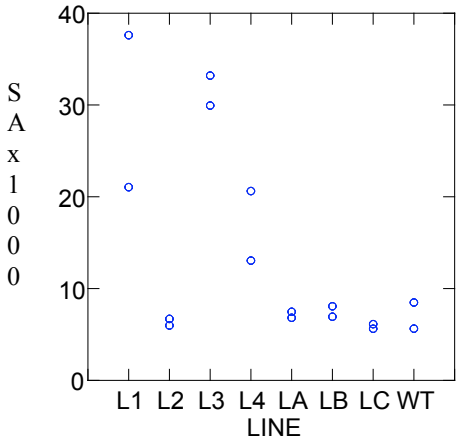

Figure 53. 35S-transgenic Arabidopsis scatter plot of NADP-ME activity measurement data. Y-axis indicates enzyme specific activity x 1000. WT = Wild-type, L1-L4 = 35S-Transgenic line, LA-LC = 35S-Empty Vector Line.

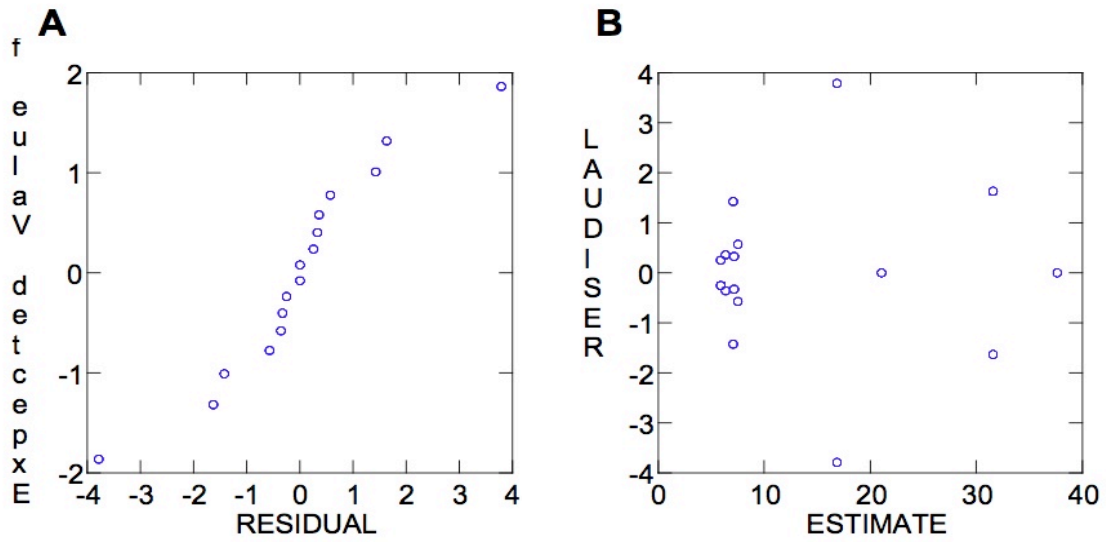

Figure 54. Confirmation of ANOVA assumptions for 35S enzyme activity. A, Probability plot of the enzyme activity data form all 35S-transgenic lines and wild-type Arabidopsis populations. This indicated a relatively normal population distribution. B, Plot assessed variance among 35S-transgenic lines and wild-type Arabidopsis populations. This indicated that the populations had relatively equal

With the assumptions confirmed, the ANOVA output was considered robust, with n = 16. Figure 55 presents the results of ANOVA, which indicated that the calculated $p < \alpha = 0.05$; therefore, the H_o is rejected ($p < 0.001$). ANOVA indicated that there was a statistical difference among the groups, but a pair-wise comparison was necessary to determine which lines had a statistically significant difference relative to wild-type.

Source	Sum-of-Squares	df	Mean-Square	F-ratio	P
LINE$	1627.48887	7	232.49841	10.54274	0.00175
Error	176.42348	8	22.05294		

Figure 55. ANOVA output for the 35S-transgenic and wild-type enzyme activity measurements. The H_o was rejected ($p < 0.001$), indicating that there were statistically significant enzyme activity differences among transgenic line relative to wild-type.

Dunnett's pair-wise comparison test indicated which lines exhibit a statistically significant difference relative to the wild-type (Fig. 56). The wild-type was set as the control and significance was detected in one direction, i.e. enzyme activity greater than WT. Enzyme activity measurements for 35S-transgenic line 1 ($p < 0.01$) and 35S-transgenic line 3 ($p < 0.01$) were statistically significant relative to the wild-type (Fig. 56). As a result, the alternative hypothesis (H_a: Transgenic enzyme activity > Wild-type enzyme activity) was not rejected for 35S-transgenic lines 1 and 3. The null hypothesis (H_o: Transgenic enzyme activity = Wild-type enzyme activity) was not rejected for all other lines. 35S transgenic plants did indicate a statistically significant elevation in NADP-ME activity relative to wild-type Arabidopsis.

Dunnett one- sided test.

Matrix of pairwise comparison probabilities:

Transgenic Line	P-value
L1	0.0036
L2	0.5000
L3	0.0020
L4	0.1354
LA	0.5000
LB	0.5000
LC	0.4999
WT	1.0000

Figure 56. Dunnett's pair wise comparison test results for 35S-transgenic and wild-type Arabidopsis. Enzyme activity measurements for 35S-transgenic line 1 ($p < 0.01$) and 35S-transgenic line 3 ($p < 0.01$) were significantly different relative to wild-type.

DISCUSSION

The overall goal for this study was to analyze the effects of over-expressing maize NADP-ME in transgenic Arabidopsis with either a KAT2 promoter directing expression in guard cells or a 35S promoter driving constitutive expression. This study was built on previous research indicating altered stomatal function in transgenic tobacco with an engineered constitutive expression of maize NADP-ME (Laporte et al., 2002). A main objective was to observe the effects of different NADP-ME expression levels and patterns caused by employing two different promoter-driven constructs. Based on preliminary SEM data, it was hypothesized that elevated, KAT2 directed expression of maize NADP-ME activity would not affect stomatal morphology but may elevate stomatal density by altering stomatal biochemistry. The control of stomatal density by malate or NADP-ME may represent a putative approach for influencing stomatal development. To expand the KAT2 transgenic plant analysis, transgenic 35S plants were also studied to determine how different expression levels and patterns affect stomatal density. A second critical aspect of this study was to provide transgene expression and enzyme activity evidence via western blots, tissue blot assays, and spectrophotometric assays. Ultimately, the observed phenotype data may be correlated to the biochemical data to indicate malate as the biological marker influencing stomatal movements and development.

The SEM investigation indicated that over-expressing NADP-ME did not affect stomatal morphology in either 35S or KAT2 transgenic Arabidopsis. However, analysis of fully expanded, older KAT2 leaves indicated that there was a statistically significant stomatal density elevation relative to wild-type Arabidopsis (Fig. 22). These data

indicated that elevated NADP-ME expression in guard cells might influence stomatal density. The mechanism is unknown, but considering the elevated activity of NADP-ME or the reduced malate concentration, either may act as a biological signal in the vast stomatal development pathway. Guard cells are believed to sense CO_2 levels because they optimize water use efficiency by gauging mesophyll CO_2 requirements while monitoring water status (Vavasseur and Raghavendra, 2005). Previous research indicated that CO_2 levels influence both stomatal movements and stomatal development. Malate, coupled with CO_2, has been suggested to influence stomatal movements, as described by the "malate hypothesis," which proposed that heightened CO_2 levels signal the release of malate from guard and mesophyll cells. Malate then triggers Cl^- and malate-permeable anion channels, causing anion release. Guard cell cation release follows, eliciting a loss in turgor, and subsequent stomatal closure (Hedrich et al., 2001). In addition, elevated CO_2 levels in Arabidopsis decreased stomatal density (Teng et al., 2006). Two of the possible explanations for my observations are that increased NADP-ME activity in the transgenic plants may have caused an internal CO_2 level surge overloading CO_2 sensors, inducing increased stomatal density, or may have reduced the internal malate concentration, inducing increased stomatal density. Either proposed mechanism may suggest malate as a biological signal for CO_2 sensing and stomatal development or the activities of NADP-ME may influence stomatal development. Further studies that measure malate and/or internal CO_2 concentrations in transgenic plants and compare those concentrations to stomatal densities may indicate a biological correlation.

However, analysis of fully expanded, younger KAT2 leaves indicated that there was not a statistically significant stomatal density difference relative to wild-type Arabidopsis

(Fig. 31). These data seem to contradict the above data, but the leaves produced early in plant development may have experienced a surge in internal CO_2 concentrations due to elevated NADP-ME activity and may have signaled for reduced stomatal density in developing leaves. Previous research demonstrated that mature leaves measure CO_2 levels by an unknown mechanism and broadcast a stomatal developmental signal directing development in young leaves (Lake et al., 2001). In addition, elevated CO_2 levels in Arabidopsis decreased stomatal density (Teng et al., 2006).

These results may be also due to different plant physiology during late-plant development versus early-plant development or the reduced activity of the KAT2 promoter during late-plant development. Pilot et al. (2001) previously detected KAT2 activity predominant in guard cells and minor veins in mature leaves. However, in developing leaves, KAT2 activity was detected in all cells, and in hypocotyls, activity was detected only in guard cells (Pilot et al., 2001). Perhaps the leaves utilized were not truly mature but still developing, and the localized guard cell NADP-ME expression was a prerequisite for the observed stomatal density elevation.

In addition, stomatal counts on fully expanded 35S transgenic younger and older leaves indicated that there was not a statistically significant stomatal density difference relative to wild-type Arabidopsis (Fig. 27 and Fig. 35). This may indicate a gradient effect in regards to NADP-ME expression patterns. Possibly guard-cell localized and elevated NADP-ME expression may influence stomatal development. Future experiments may include the analysis of more individuals to increase the sample size and NADP-ME knockout transgenic plants to determine the affect on stomatal density.

A recent, preliminary study created and studied phosphoenol pyruvate carboxylase (PEPC) deficient transgenic *Amaranthus edulis*. PEPC utilizes bicarbonate to catalyze the beta-carboxylation of phosphoenolpyruvate (PEP) to oxaloacetate, which is enzymatically converted to malate. Their results indicated that transgenic plants with severed PEPC activity and thus a low malate concentration resulted in elevated stomatal density. These results are consistent with the present study's results; both indicate increased stomatal density when malate concentration is reduced (Susanne von Caemmerer, personal communication).

The choice of preservative indicated that fixing specimens in 70% ethanol worked best. The 2.5% paraformaldehyde and 5% glutaraldehyde in 0.05 M phosphate buffer (pH 7.0) preservative did not fix the tissue well, presumably because the buffer osmolarity did not match the specimen's osmolarity. It appears that ethanol fixed the tissue much better than conventional methods. As a result, this method also greatly improved the speed and efficiency of preserving Arabidopsis specimens while limiting preservative artifacts.

The RT-PCR confirmed the presence of the maize ME gene transcript in both KAT2 and 35S whole leaf plant samples (Fig. 39 and 40). The NADP-ME enzyme assays, measuring the formation of NADPH, indicated increased enzyme activity in 2 35S-transgenic lines relative to wild-type when the absorbance was measured at 340 nm. Analysis of the KAT2 plants indicated an elevation in enzyme activity relative to wild-type; however, the difference was not statistically significant (Fig. 48). Enzyme activity may be difficult to detect because guard cells make up a very small percentage of the total leaf volume. As a result, additional assays must be conducted on a larger sample

size. The enzyme assays on the 35S plants indicated a statistically significant ($p < 0.05$) increase in enzyme activity relative to wild-type in two transgenic lines (Fig. 52). Since the 35S promoter drives constitutive expression, the activity is much more easily detected. Future studies may include determining if there is a correlation between NADP-ME activity/malate concentration and stomatal density. These preliminary data, coupled with the RT-PCR data, possibly indicate that the transcribed ME gene is active in the transgenic plants, particularly in the 35S transgenic plants.

The western blot investigation failed to detect the presence of the enzyme in both 35S and KAT2 protein extractions (Fig. 43). There may be a problem with the accessibility of the tag to the primary antibody when it folds in the plant. In addition, the primary antibody did not detect NADP-ME in protein extracted from GCP samples. The limit of detection (Fig. 44) was determined to be less than 250 ng, making the system quite sensitive. Future work includes addressing this methodological issue by removing RuBisCo from the extracted protein since it cross-reacted with the primary antibody or utilizing a different anti-penta-histidine antibody. This methodological issue fails to provide robust evidence to support the hypothesis that NADP-ME may influence stomatal density. A crucial requirement to support the hypothesis that NADP-ME/malate may influence stomatal development is to provide robust enzyme localization evidence for the transgenic plants indicating elevated, guard cell specific NADP-ME expression.

The results from the tissue blot assay (Fig. 45) indicated NADP-ME activity in protein extracted from 35S and KAT2 transgenic plants and wild-type Arabidopsis. Detection of activity in wild-type is expected because the enzyme is ubiquitous throughout nature. This approach may be ineffective in this situation because it lacks high specificity to the

maize ME. To circumvent this, GCPs may be utilized from both wild-type and KAT2 transgenic samples because of the localized expression to provide transgene expression evidence.

Future work includes a detailed phenotype analysis of the transgenic plants. A detailed gas exchange analysis is required in order to assess the hypothesis regarding over-expression of NADP-ME and its effects upon stomatal conductance and stomatal development. It is important to determine how stomatal conductance is affected as stomatal density increases. Stomatal conductance measurements were previously done on NADP-ME transformed tobacco plants (Laporte et al., 2002), and the same protocol was followed for the transgenic Arabidopsis plants. In brief, stomatal conductance was measured with a LiCor 6400 Photosynthesis System (LiCor Corp., Lincoln, Nebraska), equipped with a CO_2 mixer and integrated LED light. This instrument measures absolute concentrations of both CO_2 and H_20 in the Arabidopsis chamber by infrared gas analyzer sensors. Preliminary data from this ongoing experiment indicated that there is no difference in stomatal conductance relative to wild-type for the KAT2 and 35S transgenic plants. Even when the stomatal density was elevated, as in the KAT2 plants, there was no detected change in stomatal conductance relative to wild-type. Considering the small sample size, further analysis is required (Christine Notis, personal communication).

The main objective of this study was to continue to analyze and determine the effects of over-expressing maize NADP-ME either in guard cells or constitutively. This study suggests additional analyses to determine whether over-expressing NADP-ME in guard cells influences stomatal development. Preliminary enzyme transgene expression and enzyme activity evidence was presented, indicating that the maize ME gene was

transcribed and is active in 2 transgenic 35S plant lines. Suggested future studies include additional stomatal counts, the effect of NADP-ME inhibition, measuring malate concentrations and determining if they correlate with stomatal density, the need for more robust enzyme localization evidence, and further phenotype analysis.

The results of this research may be used to improve water use efficiency of crop plants in order to increase agricultural yields. This may be accomplished by manipulating stomatal biochemistry and/or stomatal development. Altering NADP-ME expression levels may usher in new plant biotechnologies to solve the world's growing energy and food needs.

LITERATURE CITED

Ache P, Becker D, Ivashikina N, Dietrich P, Roelfsema MRG, Hedrich R (2000) GORK, a delayed outward rectifier expressed in guard cells of *Arabidopsis thaliana*, is a K+-selective, K+-sensing ion channel. FEBS Letters **486:** 93–98

Anderson JA, Huprikar SS, Kochian LV, Lucas WJ, Gaber RF (1992) Functional expression of a probable *Arabidopsis thaliana* potassium channel in *Saccharomyces cerevisiae*. Proceedings of the National Academy of Sciences, USA **89:** 3736–3740

Artus N, Edwards G (1985) NAD-malic enzyme from plants. FEBS Lett 182: 225–233

Benfey PN, Chua NH (1989) Regulated genes in transgenic plants. Science **244**: 174-181

Berger D, Altmann T (2000) A subtilisin-like serine protease involved in the regulation of stomatal density and distribution in *Arabidopsis thaliana*. Genes and Development **14**: 1119–1131

Bergmann DC (2004) Integrating signals in stomatal development. Curr Opin Plant Biology **7:** 26-32

Blatt MR (2000) Ca^{+} signaling and control of guard-cell volume in stomatal movements. Curr Opin Plant Biology **3:** 196-204

Boudolf V, Barroco R, Engler JA, Verkest A, Beeckman T, Naudts M, Inze D, De Veylder L (2004) B1-Type Cyclin-Dependent Kinases Are Essential for the Formation of Stomatal Complexes in *Arabidopsis thaliana.* The Plant Cell **16:** 945–955

British Petroleum (2006) BP statistical review of world energy; available at www.bp.com/liveassests/bp_internet/globalbp/globalpb_uk_english/publications/energy_

reviews_2006/STAGING/local_assests/downloads/spreadsheats/statistical_review_full_report_workbook_2006.xls

Casati P, Drincovich MF, Edwards G, Andreo C (1999) Malate metabolism by NADP-malic enzyme in plant defense. Photosynth Res **61:** 99–105

Chaerle L, Saibo N, Van Der Straeten D (2005) Tuning the pores: towards engineering plants for improved water use efficiency. Trends in Biotechnology **23:** 308-315

Chang GG, Tong L (2003) Structure and function of malic enzymes, a new class of oxidative decarboxylases. Biochemistry **42:** 12721–12733

Chaves MM, Oliveria MM (2004) Mechanisms underlying plant resilience to water deficits: prospects for water-saving agriculture. J Exp Bot **55:** 2365-2384

Chawl HS (2002) Plant biotechnology and its implications to the global society. In: Introduction to Plant Biotechnology 2nd Edition. Enfield, NH: Science Publishers, Inc. 5-7

Christodoulakis NS, Menti J, Galatis B (2002) Structure and development of stomata on the primary root of *Ceratonia siliqua L*. Botany **89:** 23–29

Clough ST, Bent AF (1998) Floral dip: a simplified method for *Agrobacterium* mediated transformation of *Arabidopsis thaliana*. The Plant J **16:** 735-743

Coupe SA, Palmer BG, Lake JA, Overy SA, Oxborough K, Woodward FI, Gray JE, Quick WP (2006) Systemic signalling of environmental cues in *Arabidopsis* leaves. J Exp Bot **57:** 329-341

Croxdale JL (2000) Stomatal patterning in angiosperms. Amer J of Bot **87:** 1069–1080

Drincovich M, Casati P, Andreo CS (2001) NADP-malic enzyme from plants: a ubiquitous enzyme involved in different metabolic pathways. FEBS Lett **490:** 1–6

Earley KW, Haag JR, Pontes O, Opper K, Juehne T, Song K, Pikaard CS (2006) Gateway-compatible vectors for plant functional genomics and proteomics. The Plant J **45:** 616–629

Edwards G, Andreo CS (1992) NADP-malic enzyme from plants. Phytochemistry **31:** 1845–1857

Fischer RA (1968) Stomatal opening: Role of potassium uptake by guard cells. Science **160:** 784–785

Fitzsimons PJ, Weyers JDB. (1986) Volume changes of *Commelina communis L*. guard cell protoplasts in response to K+, light and CO_2. Physiologia Plantarum **66:** 463–468

Gotow K, Tanaka K, Kondo N, Kobayashi K, Syono K (1985) Light activation of NADP-malate dehydrogenase in guard cell protoplasts from *Vicia faba L.* Plant Physiol **79:** 829-832

Hedrich R (2002) AtKC1, a silent *Arabidopsis* potassium channel alpha-subunit modulates root hair K^+ influx. Proceedings of the National Academy of Sciences, USA **99:** 4079–4084

Hedrich R, Neimanis S, Savchenko G, Felle HH, Kaiser WM, Heber U (2001) Changes in apoplastic pH and membrane potential in leaves in relation to stomatal responses to CO_2, malate, abscisic acid or interruption of water supply. Planta **213:** 594-601

Hedrich R, Marten I, Lohse G, Dietrich P, Winter H, Lohaus G, Heldt HW (1994) Malate-sensitive anion channels enable guard cells to sense changes in the ambient CO_2 concentration. Plant J **6:** 741–748

Heldt HW (2005) The biochemistry within the plant vacuole. In: Plant Biochemistry 3rd Edition. Oxford, UK: Elsevier Academic Press 215-219

Himmel ME, Ding SH, Johnson DK, Adney WS, Nimlos MR, Brady JW, Foust TD (2007) Biomass recalcitrance: engineering plants and enzymes for biofuels production. Science **315:** 804-807

Hofgen R, Willmitzer L (1988) Storage of competent cells for *Agrobacterium* transformation. Nucleic Acids Res **16:** 987

Hosy E, Vavasseur A, Mouline K, Dreyer I, Gaymard F, Poree F, Boucherez J, Lacombe B, Pilot G, Michard E, Gaymard F, Sentenac H, Thibaud JB (2000) A *shaker*-like K^+ channel with weak rectification is expressed in both source and sink phloem tissues of *Arabidopsis*. Plant Cell **12:** 837–851

Lai LB, Nadeau JA, Lucas J, Lee EK, Nakagawa T, Zhao L, Geisler M, Sack FD (2005) The Arabidopsis R2R3 MYB proteins FOUR LIPS and MYB88 restrict divisions late in the stomatal cell lineage. Plant Cell **17:** 2754–2767

Lake JA, Quick WP, Beerling DJ, Woodward FI (2001) Plant development: signals from mature to new leaves. Nature **411:** 154

Lance C, Rustin P (1984) The central role of malate in plant metabolism. Physiol Veg **22:** 625–641

Laporte MM, Shen B, Tarchynski MC (2002) Engineering for drought avoidance: expression of maize NADP-malic enzyme in tobacco results in altered stomatal function. J Exp Bot **53:** 699-705

Larcher W (1995) Physiological plant ecology, 3rd edition. Germany: Springer-Verlag

Lebaudy A, Bouchez D, Véry AA, Simonneau T, Thibaud JB, Sentenac H (2003) The *Arabidopsis* outward K^+ channel GORK is involved in regulation of stomatal movements and plant transpiration. Proceedings of the National Academy of Sciences, USA **100:** 5549–5554**Leonhardt N, Kwak J, Robert N, Warner D, Leonhardt G, McRobbie EAC** (1997) Signalling in guard cells and regulation of ion channel activity. J Exp Bot **48:** 515-528

MacRobbie EAC (1987) Ionic relations of guard cells. In: Zeiger E, Farquhar GD, Cowan IR, eds. Stomatal Function. Stanford, CA, USA: Stanford University Press. 125–162

Martinoia E, Rentsch D (1994) Malate compartmentation: responses to a complex metabolism. Annu Rev Plant Physiol Plant Mol Biol **45:** 447–467

Marten I, Hoth S, Deeken R, Ache P, Ketchum KA, Hoshi T, Hedrich R (1999) AKT3, a phloem-localized K^+ channel, is blocked by protons. Proceedings of the National Academy of Sciences, USA **96:** 7581–7586

Morison JIL (1987) Intercellular CO_2 concentration and stomatal response to CO_2. In: Zeiger E, Farquhar G, Cowan I, eds. Stomatal Function. Stanford, CA, USA: Stanford University Press. 229–251

Mott KA, Buckley TN (2000) Patchy stomatal conductance: emergent collective behaviour of stomata. Trends in Plant Science **5:** 258-262

Mott KA (1988) Do stomata respond to CO_2 concentrations other than intercellular? Plant Physiol **86:** 200–203

Muller-Rober B, Ellenberg J, Provart N, Willmitzer L, Busch H, Becker D, Dietrich P, Hoth S, Hedrich R (1995) Cloning and electrophysiological analysis of KST1, an

inward rectifying K^+ channel expressed in potato guard cells. EMBO Journal **14:** 2409–2416

Nadeau JA, Sack FD (2003) Stomatal development: cross talk puts mouths in place. Trends in Plant Science **8:** 294-299

Nadeau JA, Sack FD (2002) Stomatal development in *Arabidopsis*. In The Arabidopsis Book (Somerville, C. R. and Meyerowitz, E.M., eds), ASPB

Nakamura RL, McKendree WL, Hirsch RE, Sedbrook JC, Gaber RF, Sussman MR (1995) Expression of an *Arabidopsis* potassium channel gene in guard-cells. Plant Physiol **109:** 371–374

Odell JT, Nagy F, Chua NH (1985) Identification of DNA sequences required for activity of the cauliflower mosaic virus 35S promoter. Nature **313:** 810–812

Ohashi-Ito K, Bergmann DC (2006) *Arabidopsis* FAMA controls the final proliferation differentiation switch during stomatal development. The Plant Cell **18:** 2493–2505

Outlaw WH Jr, Manchester J, Brown PH (1981) High levels of malic enzyme activities in *Vicia faba L.* epidermal tissue. Plant Physiol **68:** 1047-1051

Outlaw WH, Lowry OH (1977) Organic acid and potassium accumulation in guard cells during stomatal opening. Proceedings of the National Academy of Sciences, USA **74:** 4434–4438

Paliwal GS (1967) Ontogeny of stomata in some *Cruciferae*. Can J Bot **45:** 495–500

Pei ZM, Ward JM, Harper JF, Schroeder JI (1996) A novel chloride channel in *Vicia faba* guard cell vacuoles activated by the serine/threonine kinase, CDPK. EMBO J **15:** 6564–6574

Pilot G, Lacombe B, Gaymard F, Cherel I, Boucherez J, Thibaud JB,Sentenac H (2001) Guard cell inward k channel activity in *Arabidopsis* involves expression of the twin channel subunits KAT1 and KAT2. J Biol Chem **276:** 3215-3221

Raschke K, Hedrich R, Reckmann U, Schroeder JI (1988) Exploring biophysical and biochemical components of the osmotic motor that drives stomatal movement. Botanica Acta **101:** 283–294

Raschke K, Schnabl H (1978) Availability of chloride affects the balance between potassium chloride and potassium malate in guard cells of *Vicia faba L*. Plant Physiol **62:** 84–87

Reintanz B, Szyroki A, Ivashikina N, Ache P, Godde M, Becker D, Palme K, Rite G, Raschke K (2003) Metabolite export of isolated guard cell chloroplasts of *Vica faba*. New Phytologist **159:** 15-202

Roelfsema MRG, Hedrich R (2005) In the light of stomatal opening: new insights into 'the Watergate.' New Phytologist **167:** 665-691

Rothermel BA, Nelson T (1989) Primary structure of the maize NADP-dependent malic enzyme. J Biol Chem **264:** 19587-19592

Schaaf J, Walter MH, Hess D (1995) Primary metabolism in plant defense (regulation of a bean malic enzyme gene promoter in transgenic tobacco by developmental and environmental cues). Plant Physiol **108:** 949–960

Schmidt C, Schroeder JI (1994) Anion selectivity of slow anion channels in the plasma membrane of guard cells: large nitrate permeability. Plant Physiol **106:** 383–391

Schroder J (2004) Microarray expression analyses of *Arabidopsis* guard cells and isolation of a recessive absisic acid hypersensitive protein phosphatase 2C mutant. The Plant Cell **16:** 596-615

Schroeder JI, Allen GJ, Hugouvieux V, Kwak JM, Waner D (2001) Guard cell signal transduction. Annual Rev Plant Physiol and Plant Mol Biol **52**: 627-658

Schroeder JI, Ward JM, Gassmann W (1994) Perspectives on the physiology and structure of inward-rectifying K^+ channels in higher plants. Annual Rev Biophysics Biomol Struct **23:** 441-471

Sentenac H, Bonneaud N, Minet M, Lacroute F, Salmon JM, Gaymard F, Grignon C (1992) Cloning and expression in yeast of a plant potassium-ion transport-system. Science **256:** 663–665

Smith RG, Gauthier DA, Dennis DT, Turpin DH (1992) Malate and pyruvate-dependent fatty acid synthesis in leucoplasts from developing castor endosperm. Plant Physiol **98:** 1233–1238

Sunilkumar G, Mohr L, Lopata-Finch E, Emani C, Rathore KS (2002) Developmental and tissue-specific expression of CaMV 35S promoter in cotton as revealed by GFP. Plant Mol Bio **50:** 463-474

Szyroki A, Ivashikina N, Dietrich P, Roelfsema MRG, Ache P, Reintanz B, Deeken R, Godde M, Felle HH, Steinmeyer R, Palme K, Hedrich R (2001) KAT1 is not essential for stomatal opening. Proceedings of the National Academy of Sciences, USA **98:** 2917–2921

Takeuchi Y, Akagi H, Kasamura N, Osumi M, Honda H (2000) Planta (Heidelberg) **211:** 265–274

Teng N, Wang J, Chen T, Wu X, Wang Y, Lin J (2006) Elevated CO_2 induces physiological, biochemical and structural changes in leaves of *Arabidopsis thaliana.* New Phytologist **172:** 92-103

Terada R, Shimamoto K (1990) Expression of CaMV 35S-GUS gene in transgenic rice plants. Mol. Gen. Genet. **220:** 389– 392

Thakur P (2006) Increased expression of NADP malic enzyme in guard cells of *Arabidopsis* plants. MS Thesis. Eastern Michigan University

Van Krik CA, Rashke K (1978) Presence of chloride reduces malate production in epidermis during stomatal opening. Plant Physiol **61:** 361-364

Vavasseur A, AS Raghavendra (2005) Guard cell metabolism and CO_2 sensing. New Phytologist **165:** 665–682

von Groll U, Berger D, Altmanna T (2002) The Subtilisin-Like Serine Protease SDD1 Mediates Cell-to-Cell Signaling during *Arabidopsis* Stomatal Development. The Plant Cell **14**: 1527-1539

Wang H, Ngwenyama N, Liu Y, Walker JC, Zhang S (2007) Stomatal development and patterning are regulated by environmentally responsive mitogen-activated protein kinases in *Arabidopsis.* Plant Cell **19:** 63–73

Wheeler MCG, Tronconi MA, Drincovich MF, Andreo CS Maurino (2005) A comprehensive analysis of the NADP-malic enzyme gene family of Arabidopsis. Plant Physiol **139:** 39-51

Williamson JD, Hirsch-Wyncott ME, Larkins BA, Gelvin SB (1989) Differential accumulation of a transcript driven by the CaMV 35S promoter in transgenic tobacco. Plant Physiol **90:** 1570–1576

Willmer CM, Fricker MD (1996) Stomata, 2nd edn. London, UK: Chapman & Hall.

Xiang C, Han P, Lutziger I, Wang K, Oliver DJ (1999) A mini binary vector series for plant transformation. Plant Molec Bio **40:** 711-717

Yang NS, Christou P (1990) Cell type specific expression of a CaMV 35S-GUS gene in transgenic soybean plants. Dev. Genet. **11:** 289–293